

Monitoring the plasmasphere by spacecraft observations of toroidal mode standing Alfvén waves

Kazue Takahashi

(Johns Hopkins University Applied Physics Laboratory, USA)

International School of Space Science
Radiation Belt Dynamics and Remote Sensing of the Earth's Plasmasphere

26-30 September, 2022
L'Aquila, Italy

Acknowledgements: Richard Denton (Dartmouth College)

Outline

- Introduction
- Methodology
- Data analysis results

Introduction

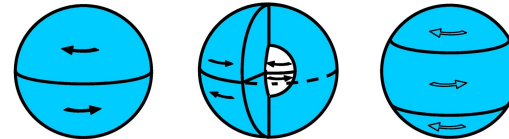
What is normal mode magnetoseismology?

- Use of the properties of observable MHD eigenmode oscillations in the magnetosphere to infer the plasma mass density
- Toroidal-mode standing Alfvén waves are the most frequently used wave mode
- Distinct from travel time magnetoseismology

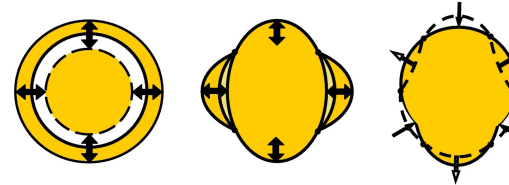
Comparison with other seismologies

- Sun and Solid Earth
 - Steady background medium
 - High-Q resonances
 - Many spectral lines
- Magnetosphere
 - Variable background medium
 - Low-Q resonances
 - Small number of observable spectral lines

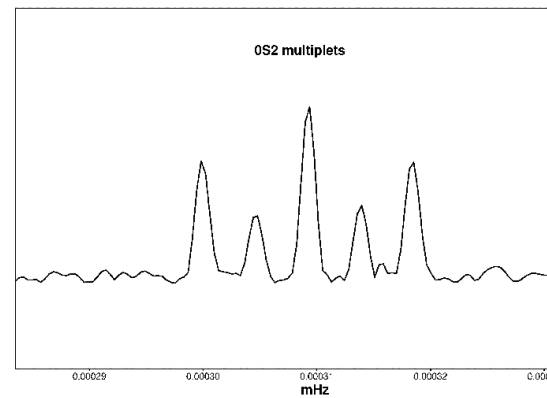
Solid Earth seismology



Toroidal modes ${}_0T_2$ (44.2 min), ${}_1T_2$ (12.6 min) and ${}_0T_3$ (28.4 min)



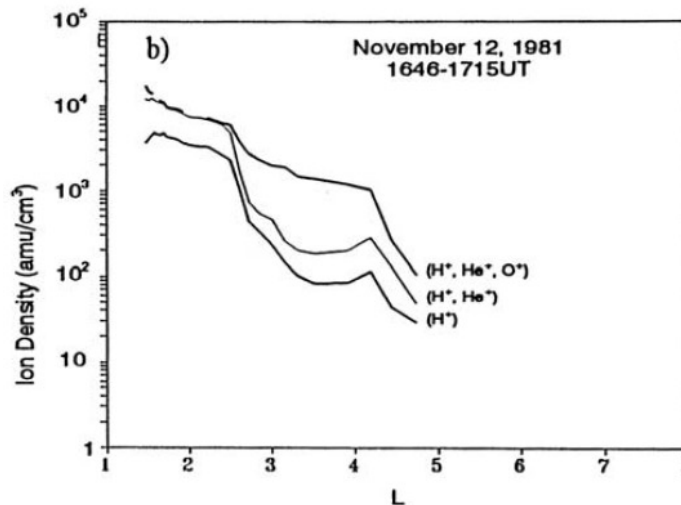
Spheroidal modes ${}_0S_0$ (20.5 min), ${}_0S_2$ (53.9 min) and ${}_0S_3$ (25.7 min)



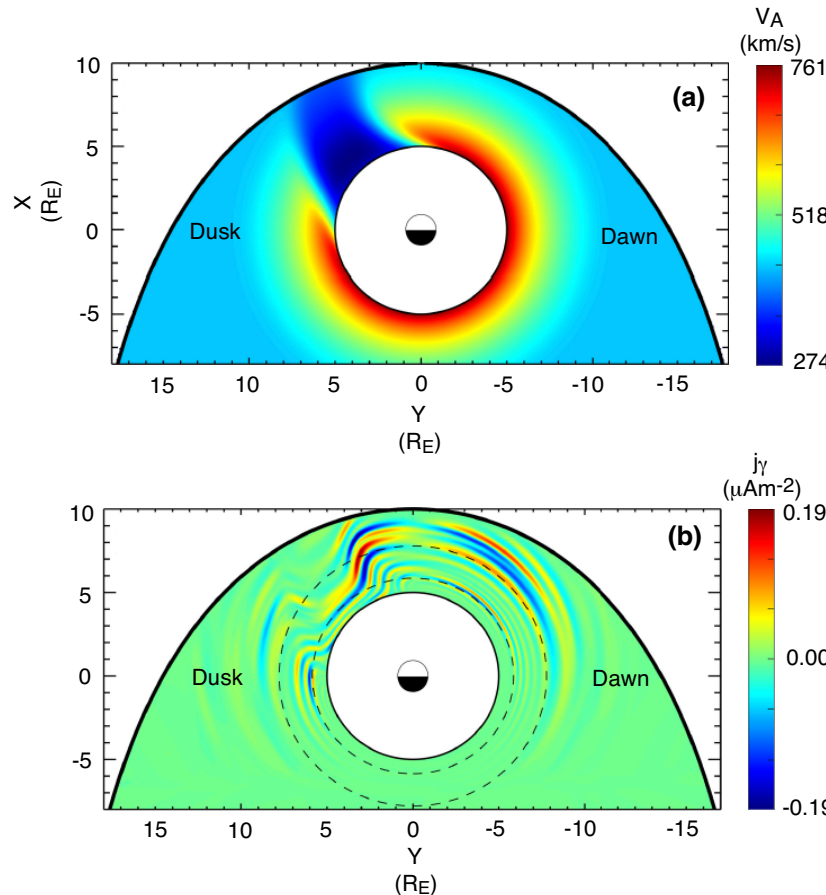
(<http://www.iris.iris.edu/sumatra/Uncompressedimages>)

Magnetoseismology science target: Where is the plasmapause?

- Magnetospheric plasma mainly consists of H^+ , He^+ , and O^+ .
 - H^+ (1 amu) carries the number density.
 - O^+ (16 amu) contributes to the mass density with high a degree of variability.
- Plasmasphere is traditionally defined in terms of the electron or H^+ density.
- But the “mass density plasmasphere” can be different when the ion composition changes with position.

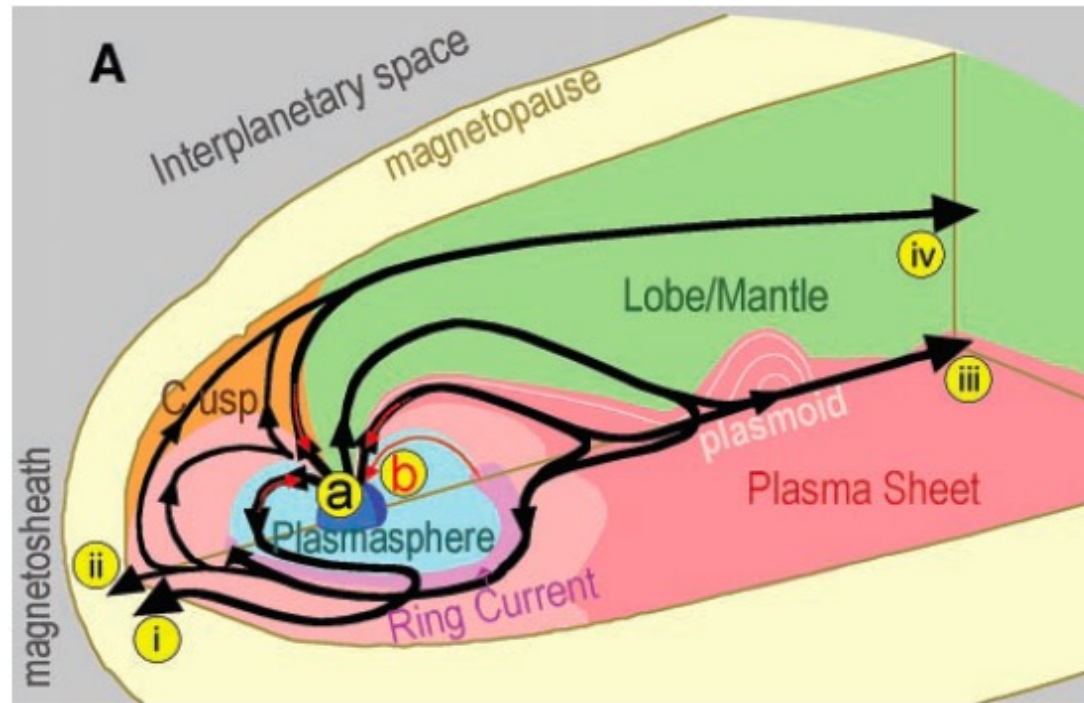


Magnetoseismology science target: How do drainage plumes alter the local and global properties of MHD waves?



(Wright and Elsden, 2020)

Magnetoseismology science target: How are ionospheric O⁺ ions transported?



(Seki et al., 2001)

Cold plasma controls various phenomena in the magnetosphere

Table 1. Cold plasma populations and their known effect on the Earth's magnetosphere.

Cold Population	Impact on the Magnetosphere
Plasmasphere ions	Alter ULF frequency and radial diffusion of energetic electrons and ions Alter EMIC scattering of electron radiation belt
Plasmasphere electrons	Alter HISS decay of radiation-belt electrons Create whistler ducts
Plasmapause	HISS-chorus boundary Site of enhanced ULF activity Site of shear-flow instabilities leading to giant undulations
Plasmaspheric plume ions	Reduce the dayside reconnection rate Alter Hall microphysics of dayside reconnection Alter EMIC scattering of outer electron radiation belt
Cloak ions	Alter ULF frequency and radial diffusion of energetic electrons and ions Reduce the dayside reconnection rate Alter Hall microphysics of dayside reconnection Alter EMIC scattering of electron radiation belt Reduce electron-plasma-sheet-driven spacecraft charging Reduce threshold for Kelvin-Helmholtz on magnetopause
Cloak electrons	Alter chorus and affect electron-radiation-belt energization
Structured dawnside cold electrons	Produce spatial structure of (a) chorus-wave amplitudes and (b) the pulsating aurora
Charge-exchange-byproduct protons	Alter Hall microphysics of dayside reconnection May increase early-time plasmaspheric refilling rate Alter EMIC scattering of electron radiation belt
Ionospheric ion outflows	Provide a major source of magnetospheric plasma
Ionospheric ion outflows in magnetotail	Alter Hall microphysics of magnetotail reconnection Mass-loading of magnetotail reconnection Alter magnetotail tearing instability
Ionospheric electron outflows	Alter chorus properties

NSF GEM Focus Group: The Impact of the Cold Plasma in Magnetospheric Physics (Gian Luca Delzanno et al.)
https://gem.epss.ucla.edu/mediawiki/index.php/FG:_The_Impact_of_the_Cold_Plasma_in_Magnetospheric_Physics

How do we determine the mass density using spacecraft?

1. Measure ion fluxes and take their moment

$$\rho = \sum_i m_i \int d\mathbf{v} f_i(\mathbf{v})$$

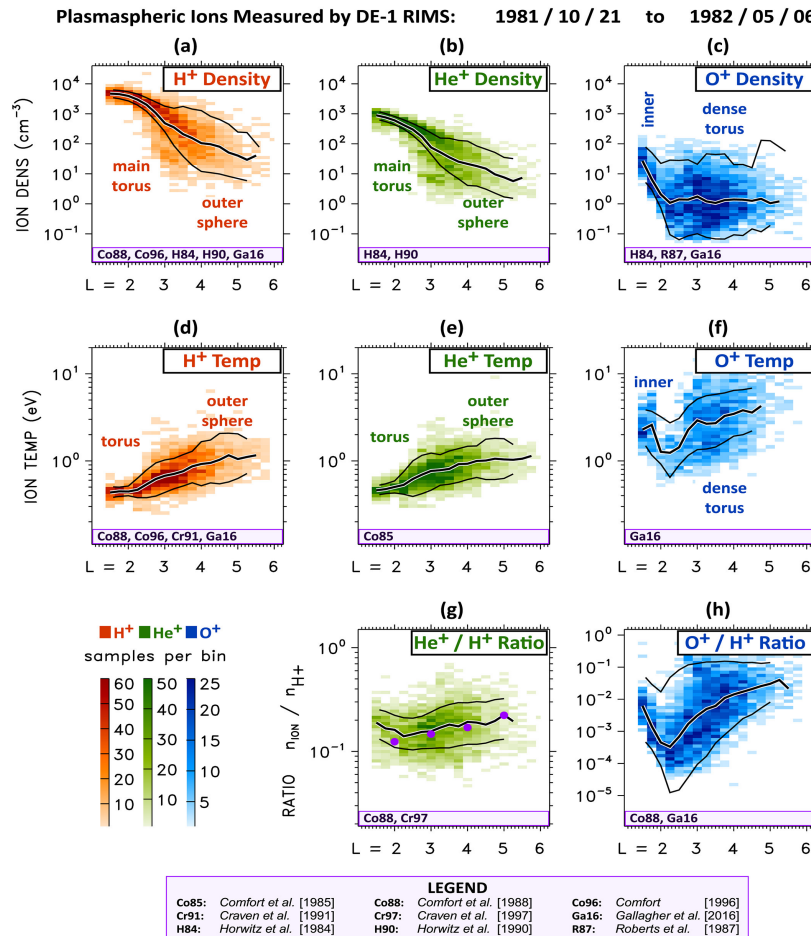
→ Difficult to capture low-energy (< 10 eV) particles, which tend to carry most of the mass density

2. Use indirect methods (normal mode magnetoseismology)

→ Relies on the presence of standing Alfvén waves

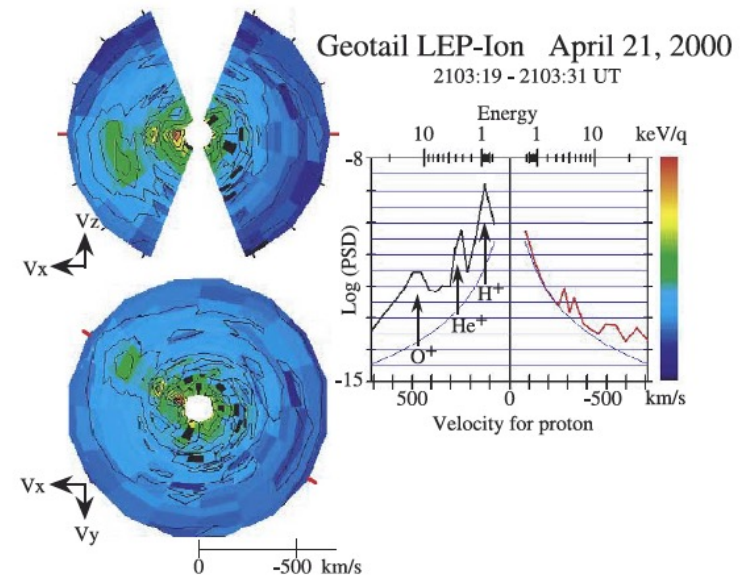
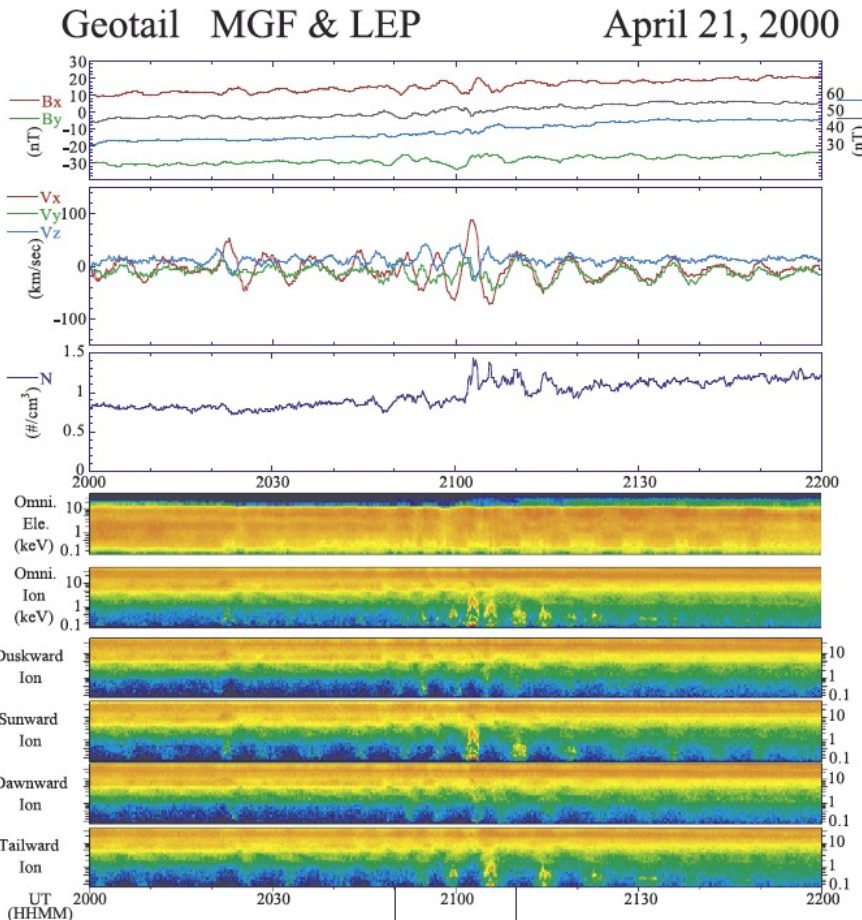
O⁺ density is highly variable

- Dynamics Explorer 1
 - 1981-1991
 - $1.8 \times 4.8 R_E$ polar orbit
- Retarding Ion Mass Spectrometer (RIMS)
 - Energy < 50 eV
 - Ion composition: 1-40 amu/charge
 - Negative potential bias



(Goldstein et al., 2019)

Particle detectors catch cold ions when there is strong bulk plasma flow



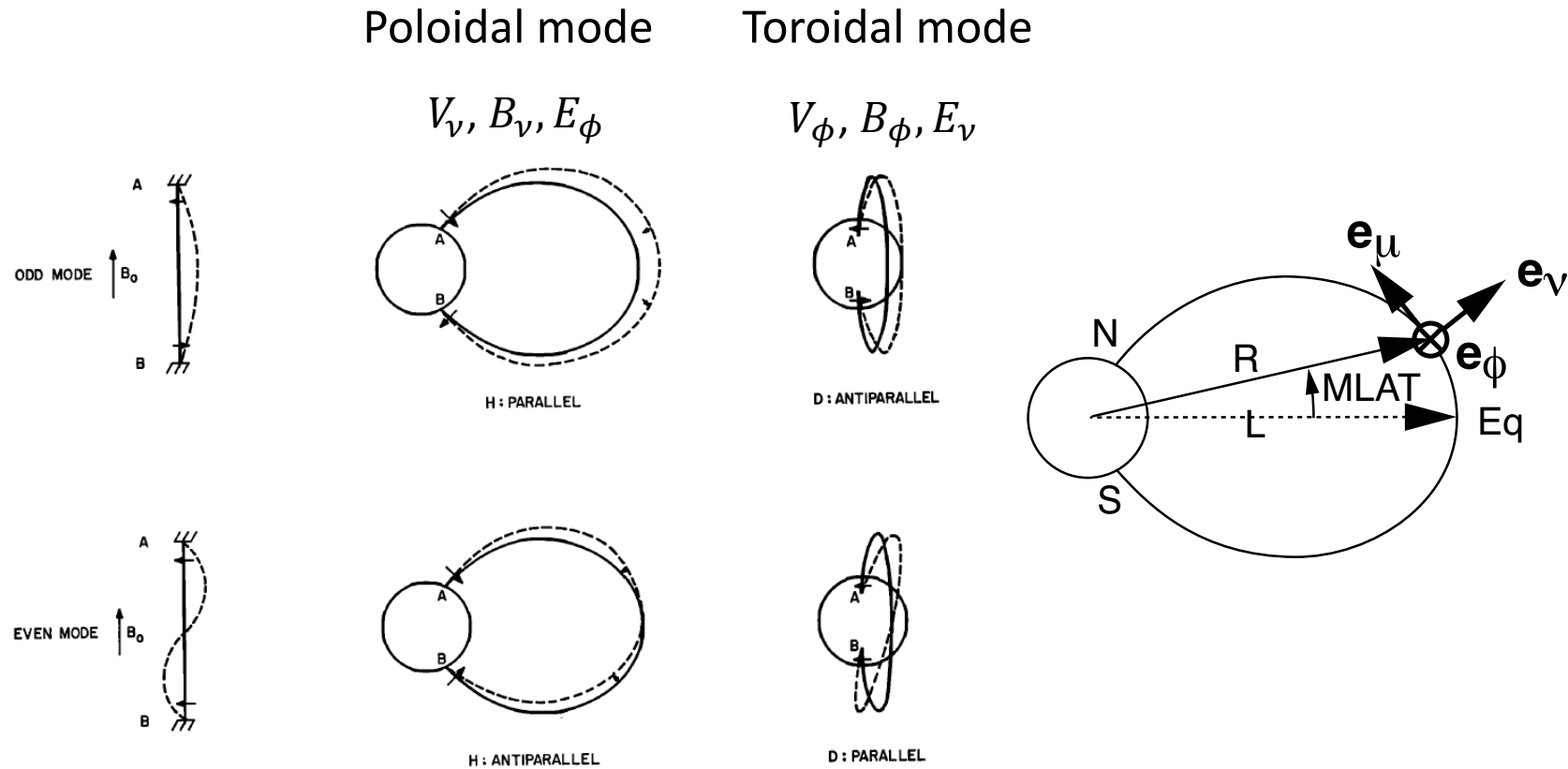
This usually does not happen in the inner magnetosphere ($L < 6$)

(Hirahara al., 2014)

Magnetoseismology : Spacecraft vs ground experiments

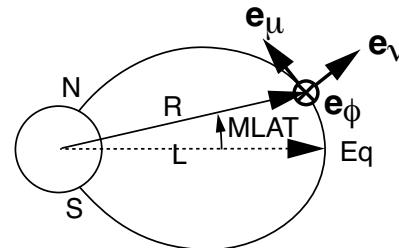
- Ground
 - Numerous permanent stations
 - Cross-phase technique is well established
 - Field line mapping to the equator is model dependent and difficult at high L
- Spacecraft
 - Continuous crossing of L shells
 - Straightforward mapping to the equator
 - Electron density available (f_{UHR})
 - Limited number of spacecraft

Standing Alfvén waves are classified by polarization and harmonic mode



(Sugiura and Wilson, 1964)

MHD wave equation for axisymmetric dipole magnetosphere provides basic Alfvén wave properties



$$\partial^2 \mathbf{E} / \partial t^2 = \mathbf{V}_A \times \mathbf{V}_A \times (\nabla \times (\nabla \times \mathbf{E}))$$

Assume incompressible modes ($\delta B_\mu = 0$) to get decoupled equations

$$H_1 \partial / \partial_\mu (H_2 \partial \epsilon_\nu / \partial_\mu) + (\omega^2 / A^2) \epsilon_\nu = 0 \quad \text{Toroidal waves}$$

$$H_2 \partial / \partial_\mu (H_1 \partial \epsilon_\phi / \partial_\mu) + (\omega^2 / A^2) \epsilon_\phi = 0 \quad \text{Poloidal waves}$$

(Cummings et al., 1969)

Decoupling is also achieved by assuming extreme azimuthal wave numbers (m)

Wave fields $\sim e^{-im\phi}$

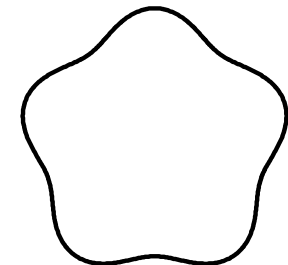
$m \rightarrow 0$

Axisymmetric toroidal mode
(Radoski and Carovillano, 1966)

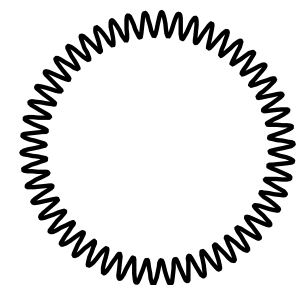
$m \rightarrow \infty$

Guided poloidal mode
(Radoski, 1967)

$m = 5$

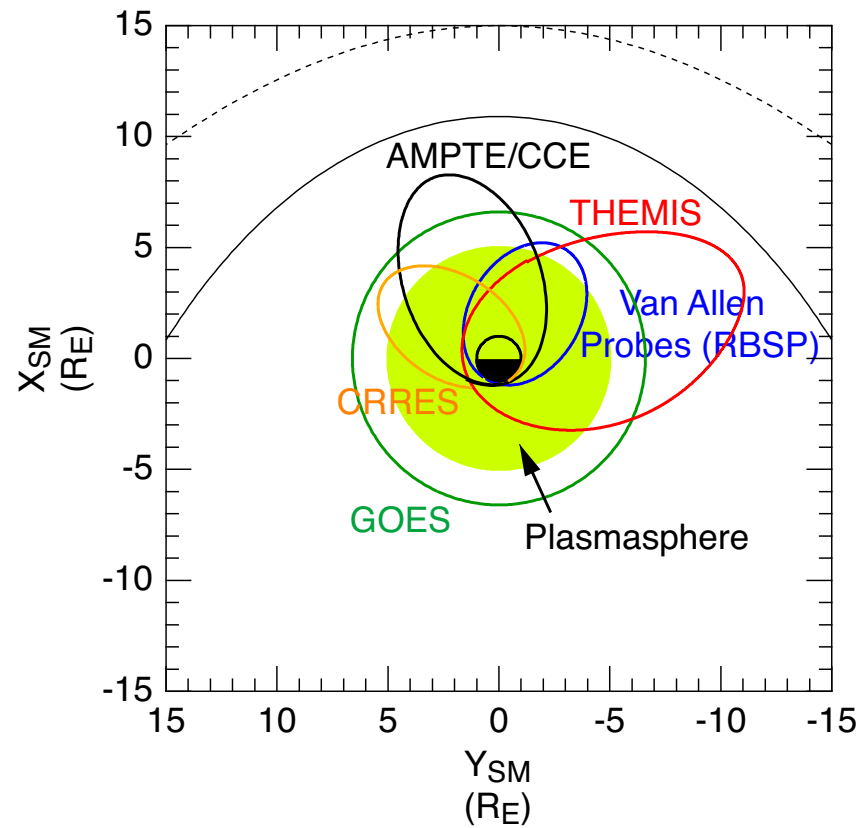


$m = 50$

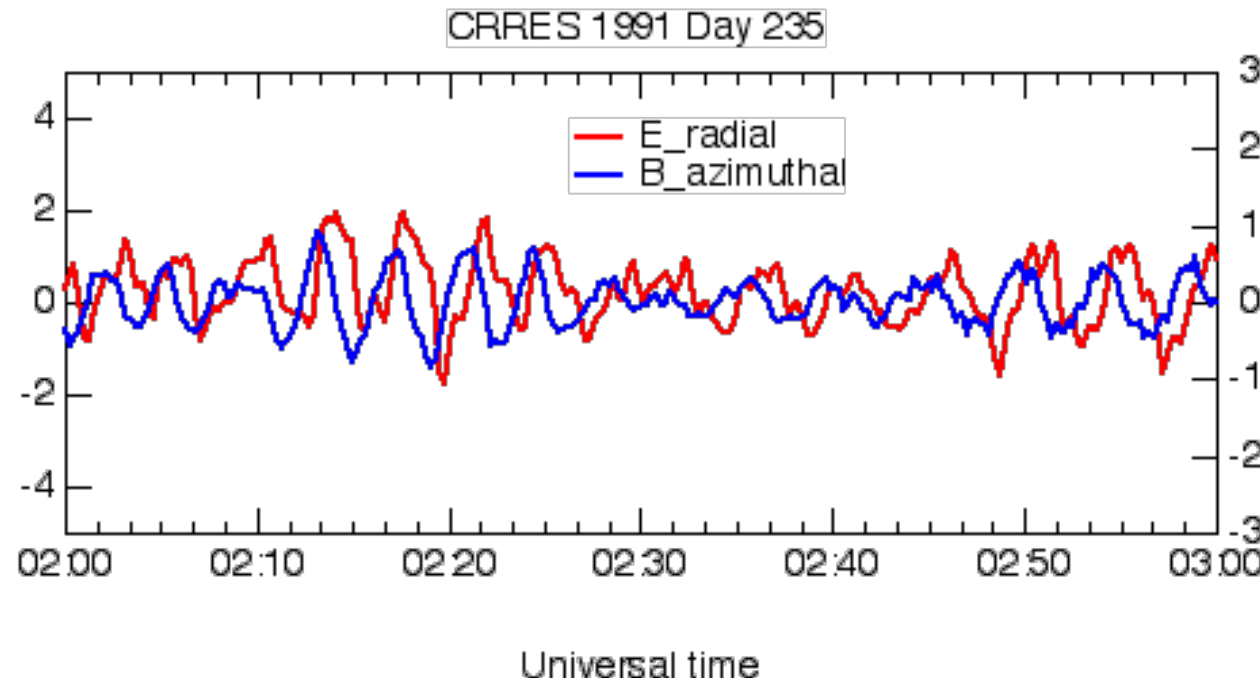


Equatorial spacecraft have been used to detect Alfvén waves

GOES	1974-Present
AMPTE/CCE	1984-1989
CRRES	1990-1991
THEMIS	2007-Present
RBSP	2012-2019



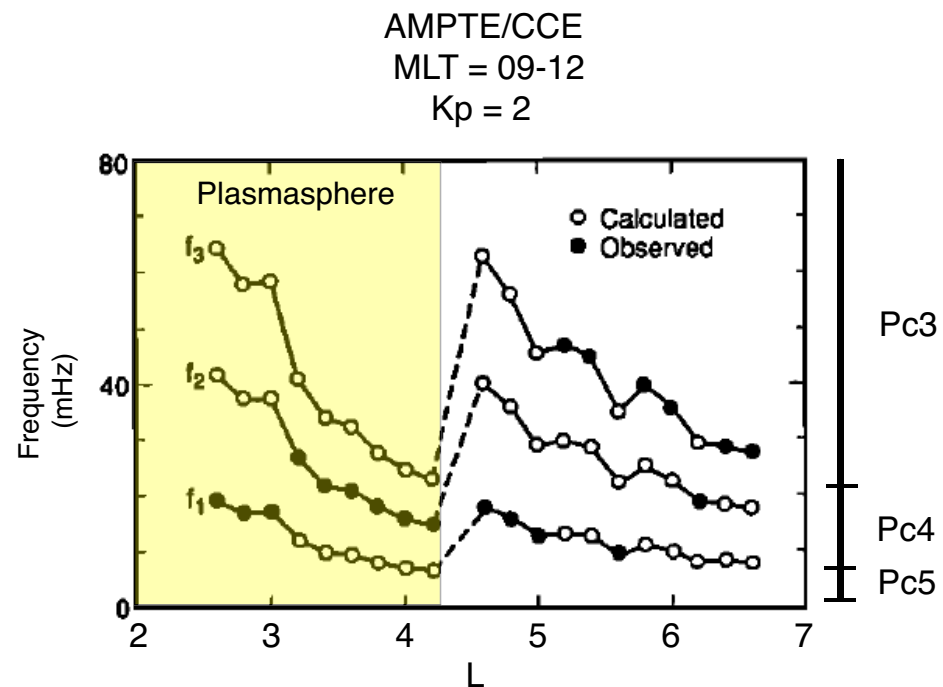
Standing Alfvén waves are sinusoidal oscillations with orthogonal E- and B-field components exhibiting a 90-degree phase delay



We have been using the same ULF wave classification scheme for ~60 years!

Notation	Period range (s)	Frequency range (mHz)
Pc1	0.2-5	200-500
Pc2	5-10	100-200
Pc3	10-45	22-100
Pc4	45-150	6.7-22
Pc5	150-600	1.7-6.7

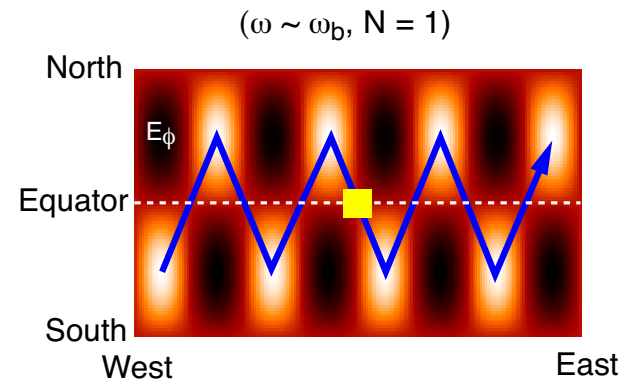
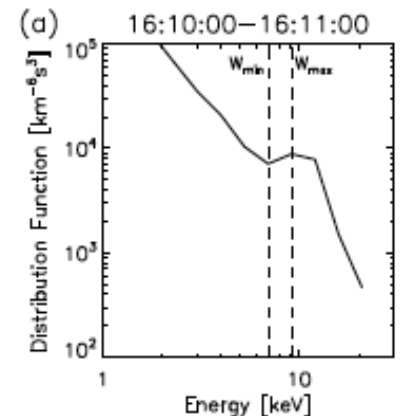
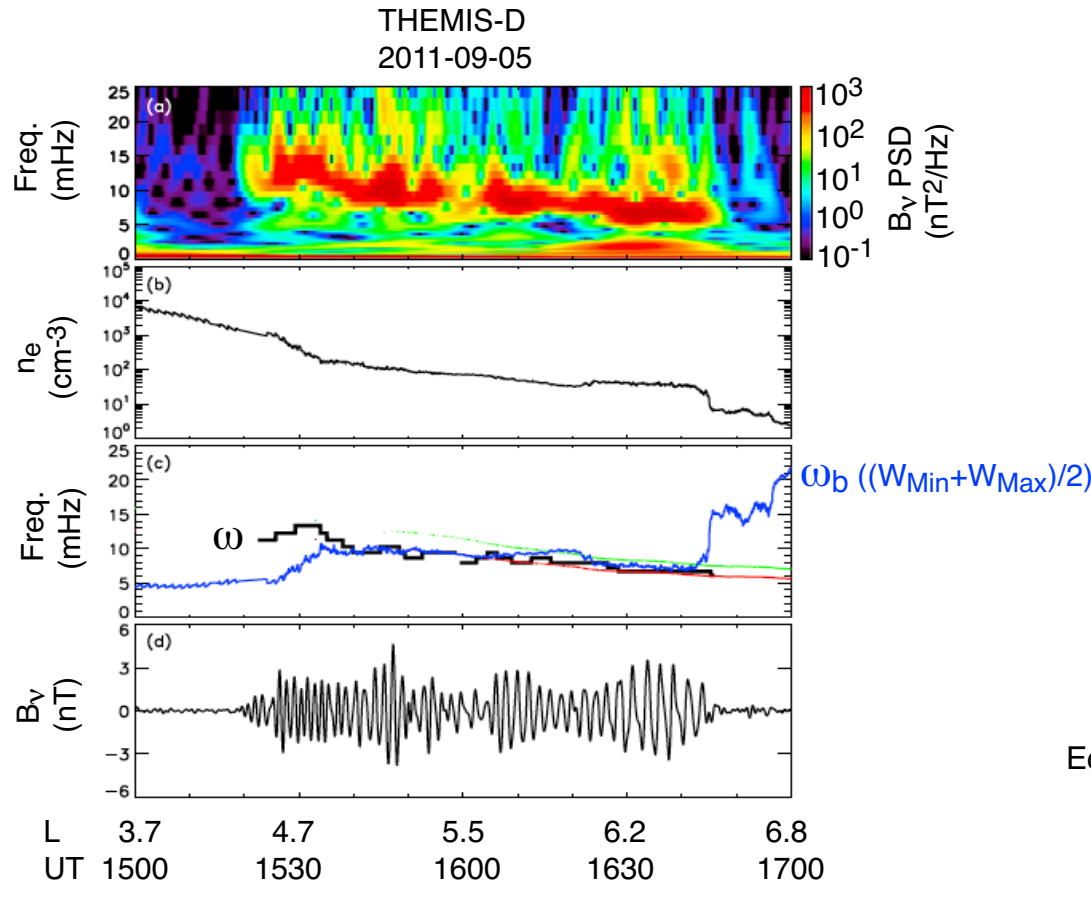
(Jacobs et al., 1964)



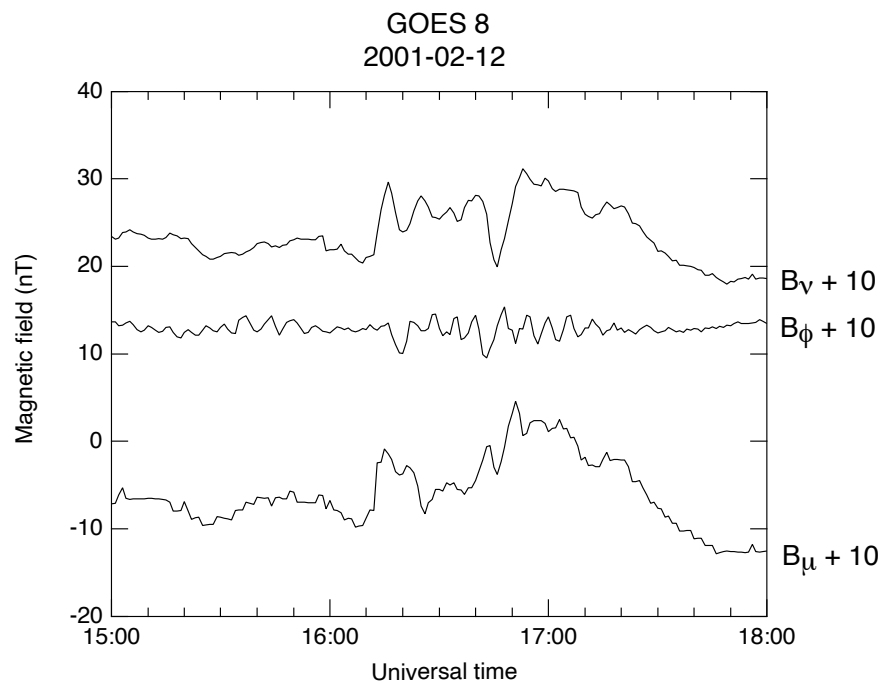
(Takahashi and Anderson., 1992)

Monochromatic poloidal Pc4 waves are excited through bounce drift resonance

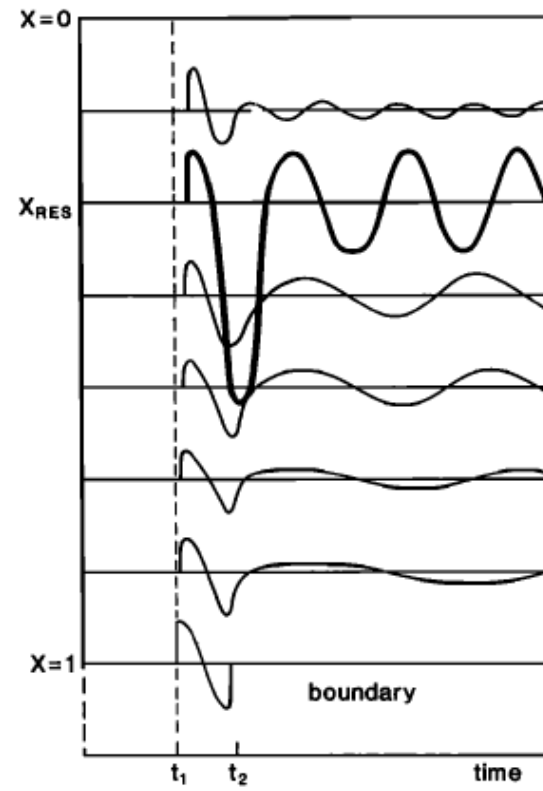
$$\omega - m\omega_d = N\omega_b$$



Toroidal Pc5 waves are excited by solar wind dynamic pressure pulses

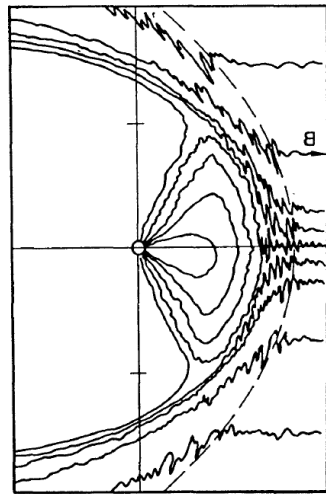


(Takahashi & Ukhorskiy., 2007)

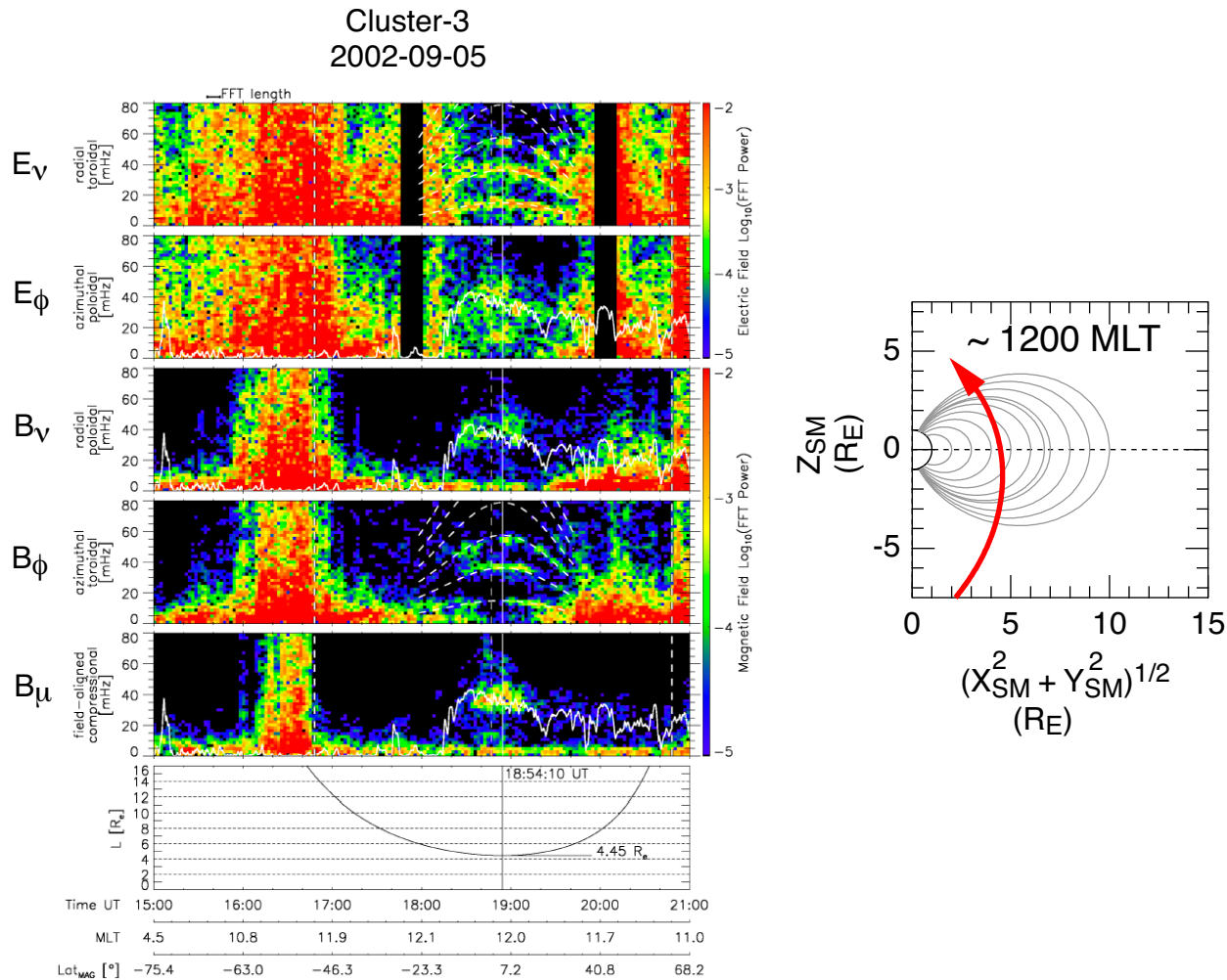


(Southwood & Kivelson., 1990)

Toroidal Pc3 waves are driven by ULF waves excited in the ion foreshock

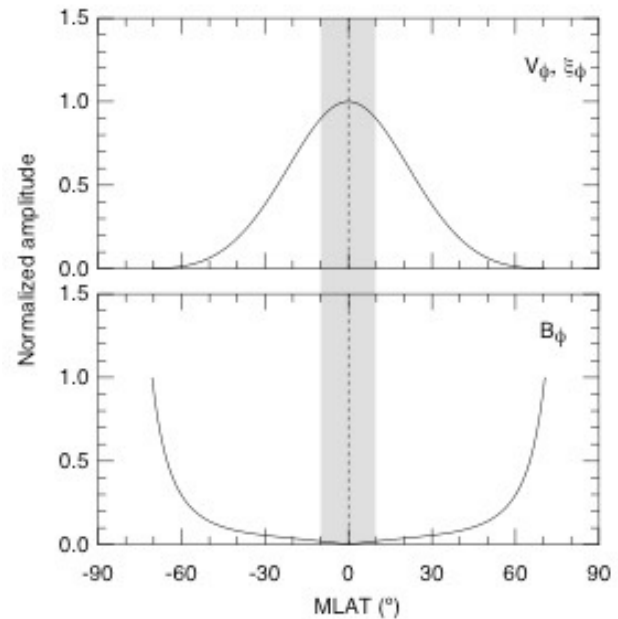
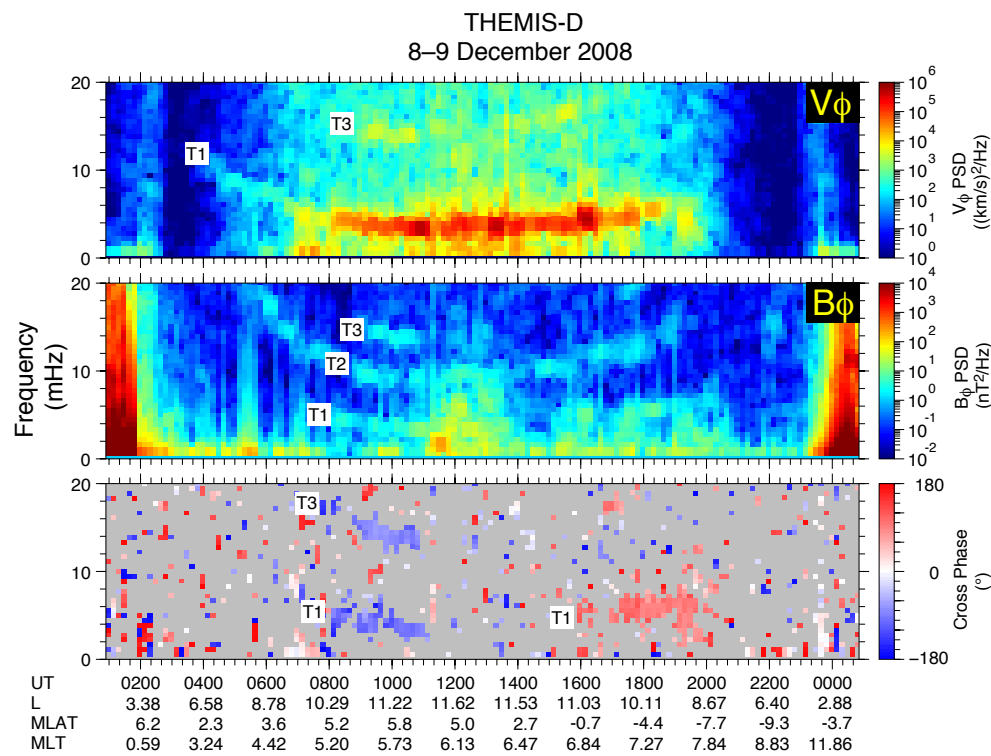


(Greenstadt et al., 1980)



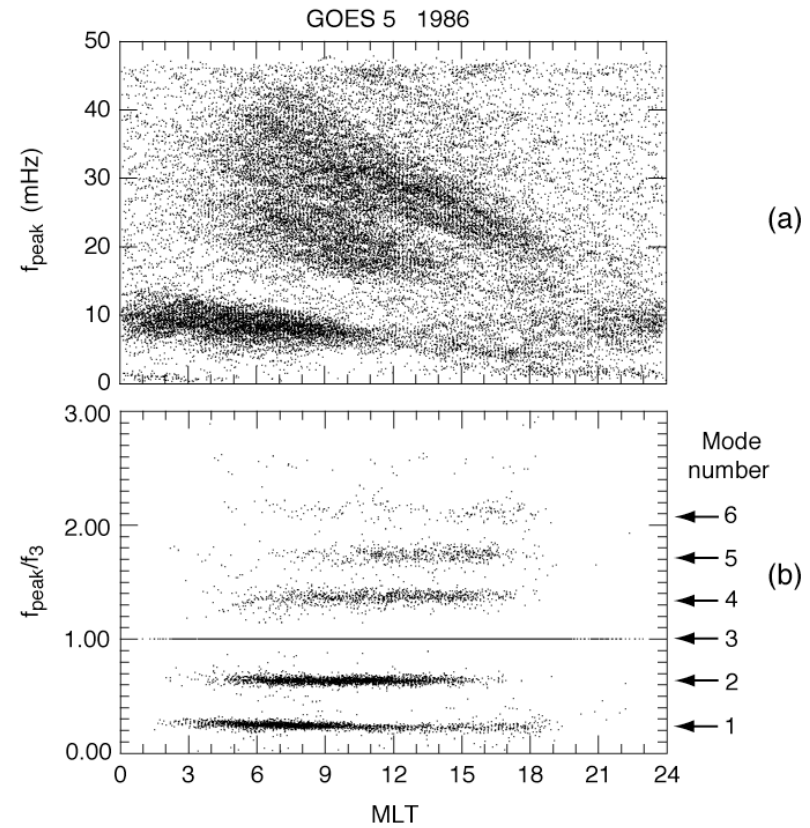
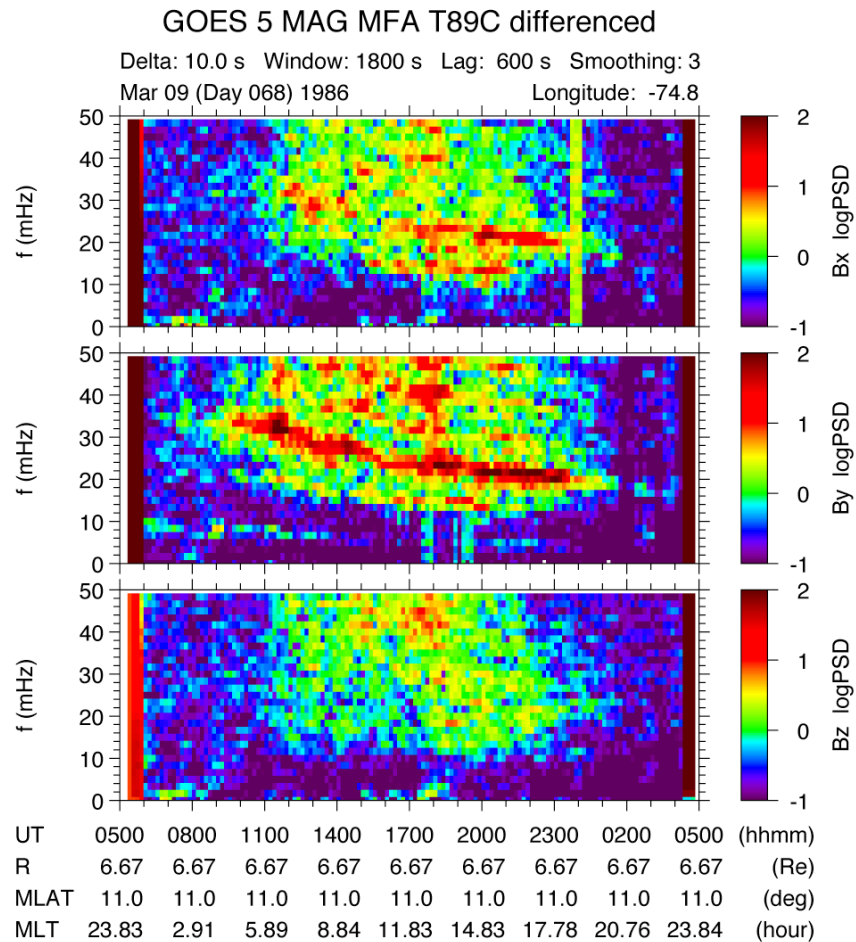
(Clausen et al., 2009)

Oscillations in ion bulk velocity often represent Pc5 toroidal waves at $L > 6$



(Takahashi et al., 2015)

Multiharmonic toroidal waves are very common on the dayside

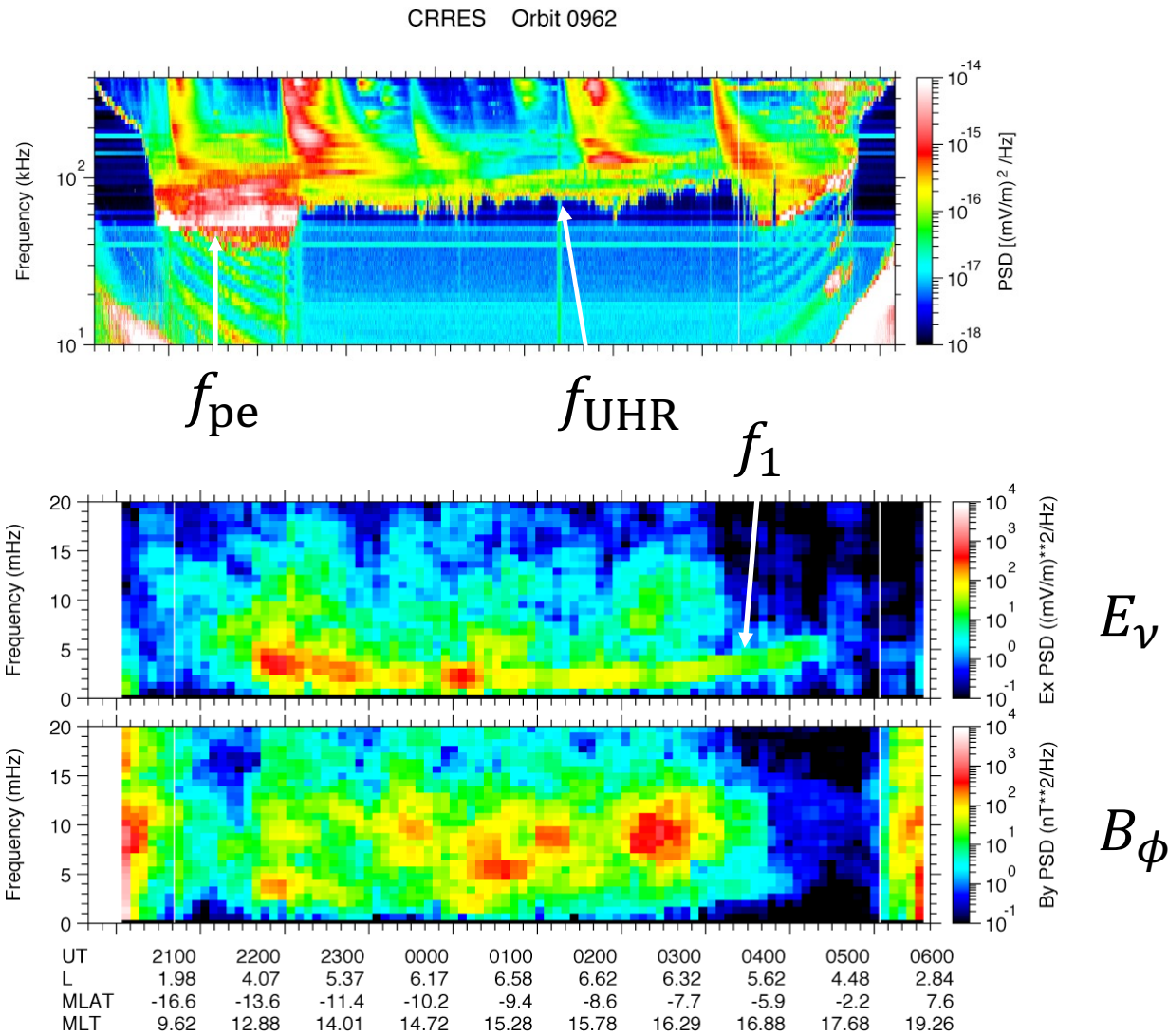


(Takahashi and Denton, 2007)

Magnetoseismic techniques

Spacecraft data used in magnetoseismology

Plasma wave spectra
→ Electron density, n_e



(Takahashi et al., 2008)

Steps of mass density analysis

1. Select a magnetic field model
2. Select a field line mass distribution model (e.g., α)
3. Solve the wave equation for a reference equatorial mass density $\rho_{\text{eq_ref}}$ (e.g., 1 amu/cc) to obtain the wave frequencies f_{n_ref} (n : harmonic number)
4. Observationally determine the wave frequencies f_{n_obs}
5. The mass density estimate is given by

$$\rho_{\text{eq_est}} = \rho_{\text{eq_ref}} (f_{n_ref}/f_{n_obs})^2$$

Average ion mass (M) is an important product of magnetoseismology

$$f^{-1} \propto \oint \frac{ds}{V_A} = \oint \frac{ds}{B\sqrt{\mu_0\rho}}$$

f : Standing Alfvén wave frequency

ρ : Mass density (from f)

n_e : Electron number density (from f_{UHR})

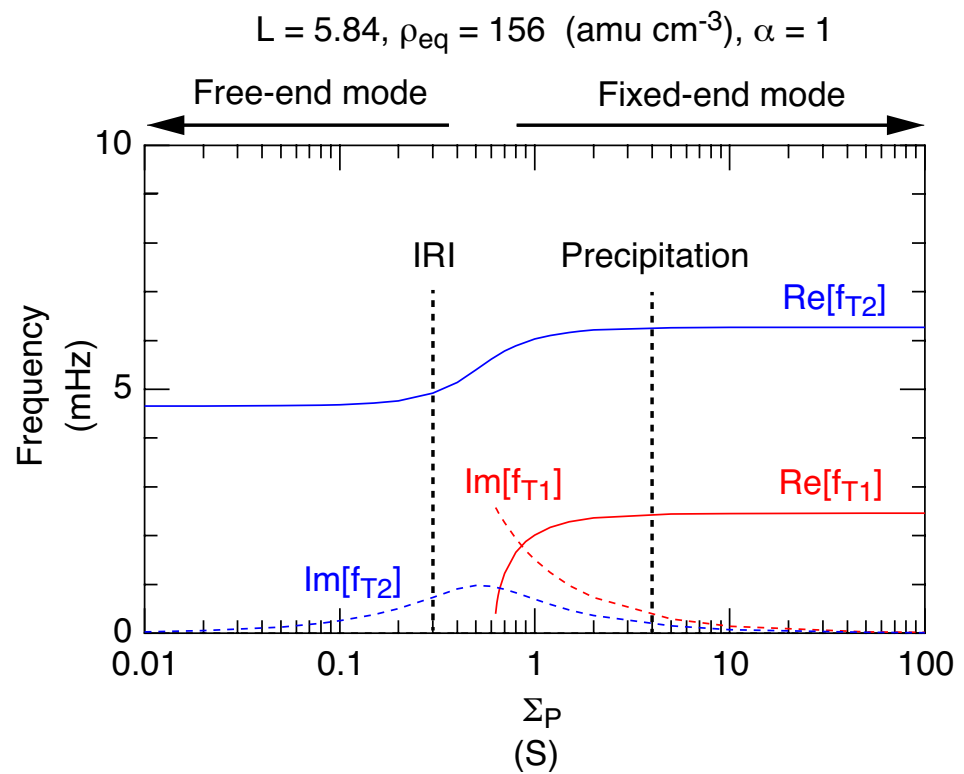
M ($= \rho/n_e$): Average ion mass → ion composition

$$\rho = n_e m_e + \sum n_i m_i \approx n_{\text{H+}} m_{\text{H+}} + n_{\text{He+}} m_{\text{He+}} + n_{\text{O+}} m_{\text{O+}} \approx n_e M$$

Ionospheric conductivity needs to be high enough to sustain fixed-end standing Alfvén waves

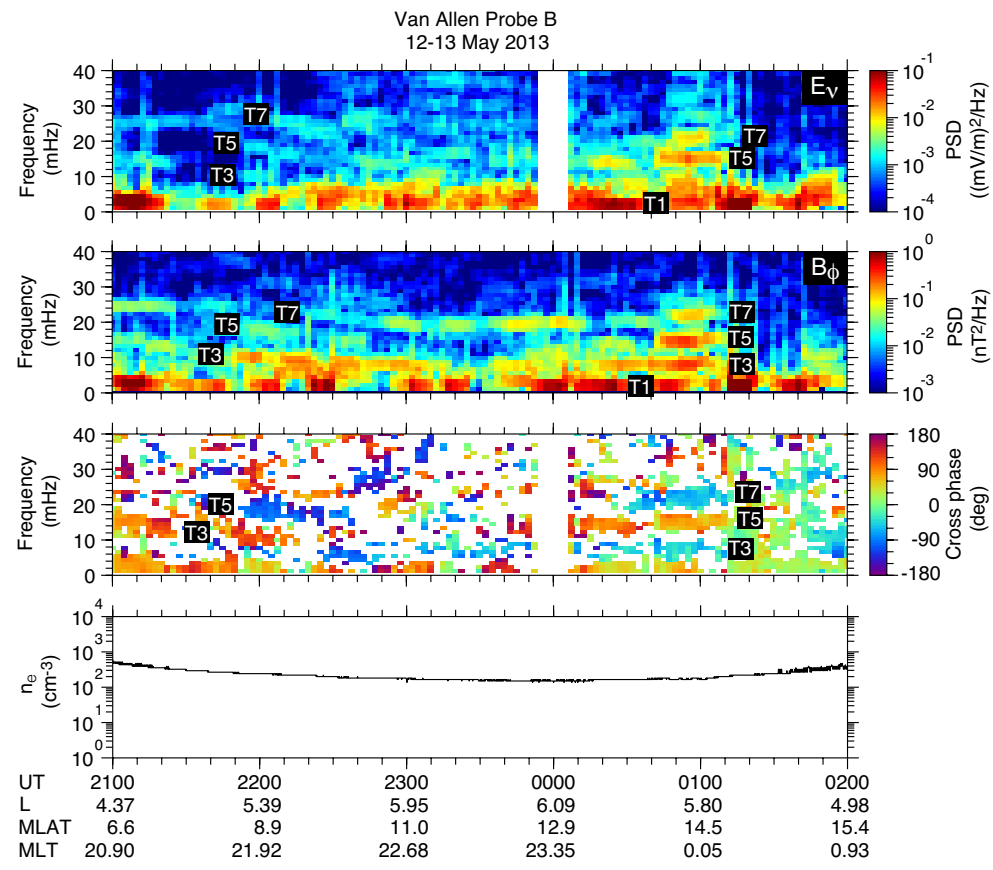
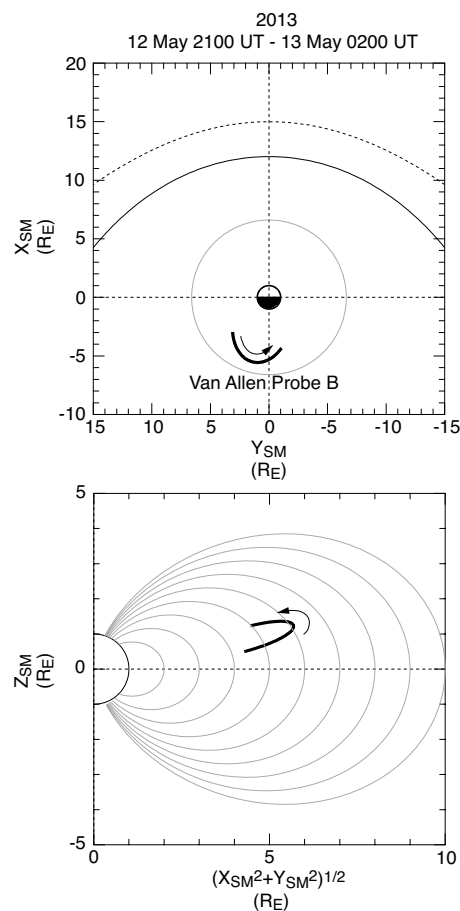
Ionospheric boundary condition

$$\delta E_\nu = \pm \frac{\delta B_\phi}{\mu_0 \Sigma_P}$$



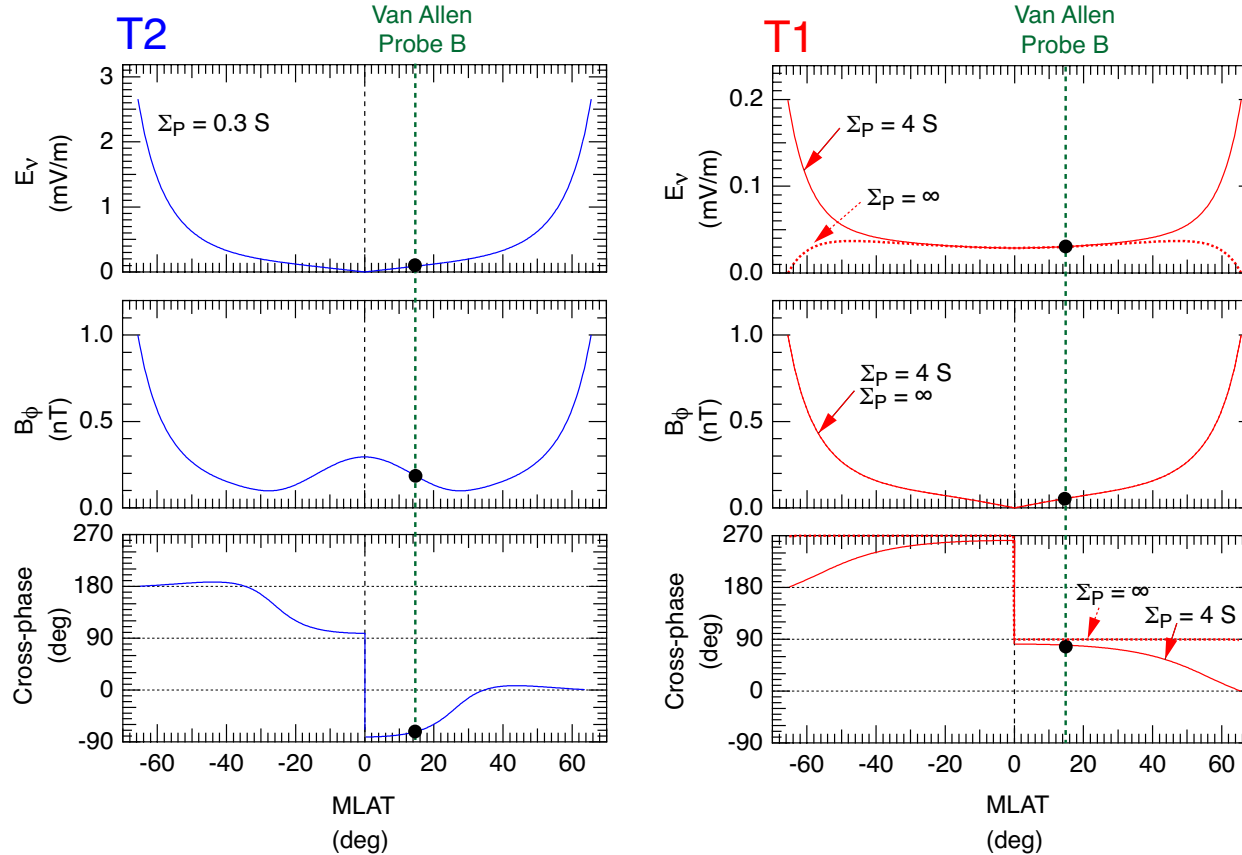
(Takahashi et al., 2020)

Ionospheric conductivity needs to be high enough to sustain fixed-end standing Alfvén waves



Observed cross-phase is consistent with fixed-end mode

$L = 5.84, \rho_{eq} = 156$ (amu cm $^{-3}$), $\alpha = 1$



(Takahashi et al., 2020)

The success of magnetoseismology depends on
the choice of models for the magnetic field and
field line mass density distribution

There is a widely used approximation for general magnetic field geometry

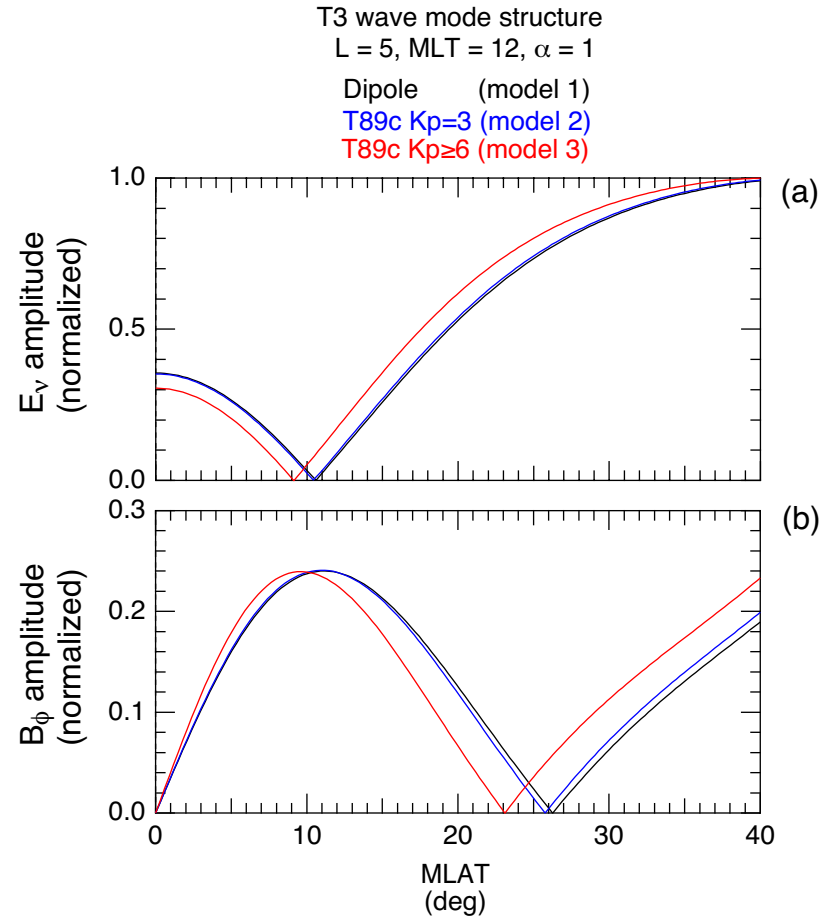
$$\mu_0 \rho \frac{\partial^2 (s_i/h_i)}{\partial t^2} = \frac{1}{h_i^2} \mathbf{B}_0 \cdot \nabla \left\{ h_i^2 [\mathbf{B}_0 \cdot \nabla (s_i/h_i)] \right\}$$

Tsyganenko models are usually good for \mathbf{B}_0

(Singer et al., 1981)

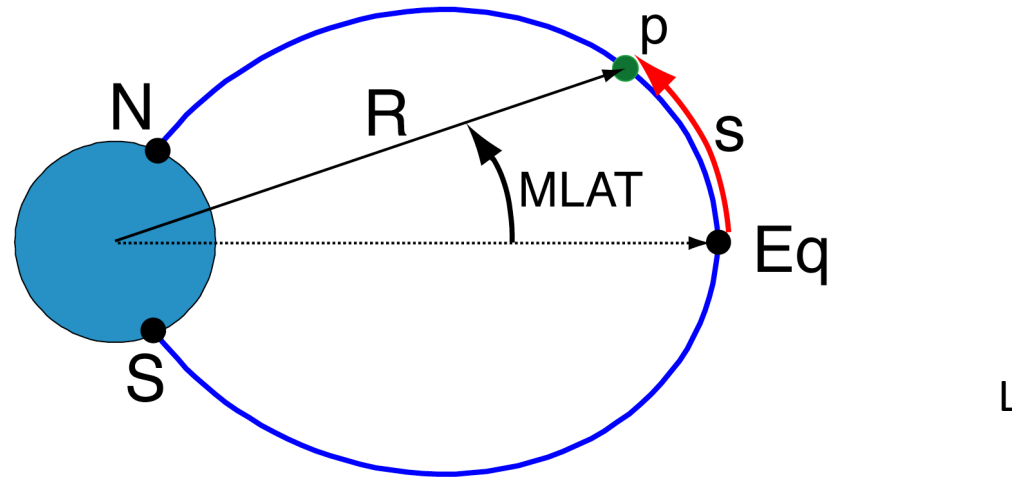
Dipole field is a good approximation in the dayside plasmasphere

- Exceptions
 - Large distances
 - High geomagnetic activity



(Takahashi & Denton, 2021)

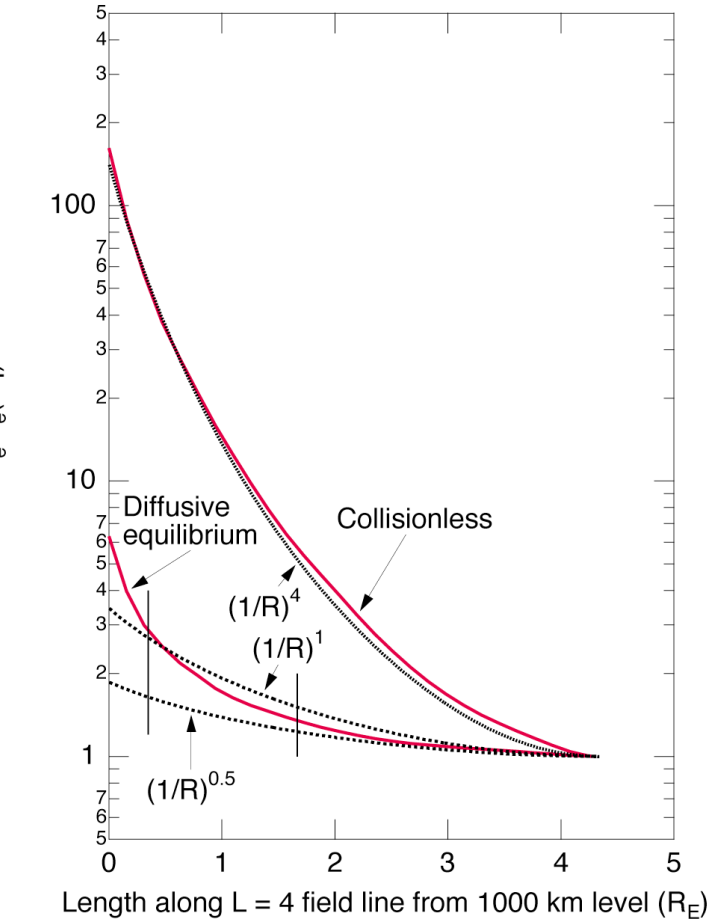
We use a very simple model for field line mass density distribution



$$\rho = \rho_{eq} \left(\frac{LR_E}{R} \right)^\alpha$$

Theoretical models of field line density distribution (H^+ plasma)

- Diffusive equilibrium
 - Plasmasphere
 - $\alpha \simeq 1$
- Collisionless distribution
 - Plasmatrough
 - $\alpha \simeq 4$



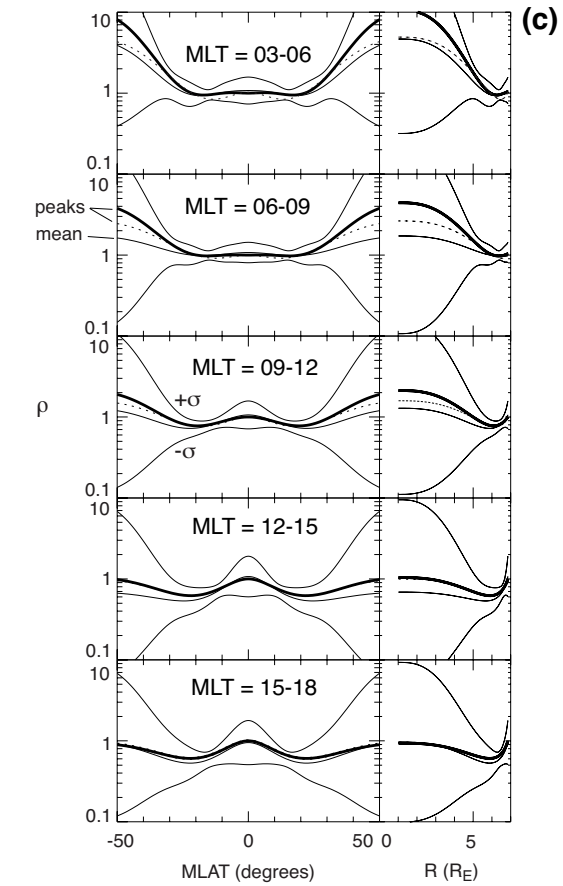
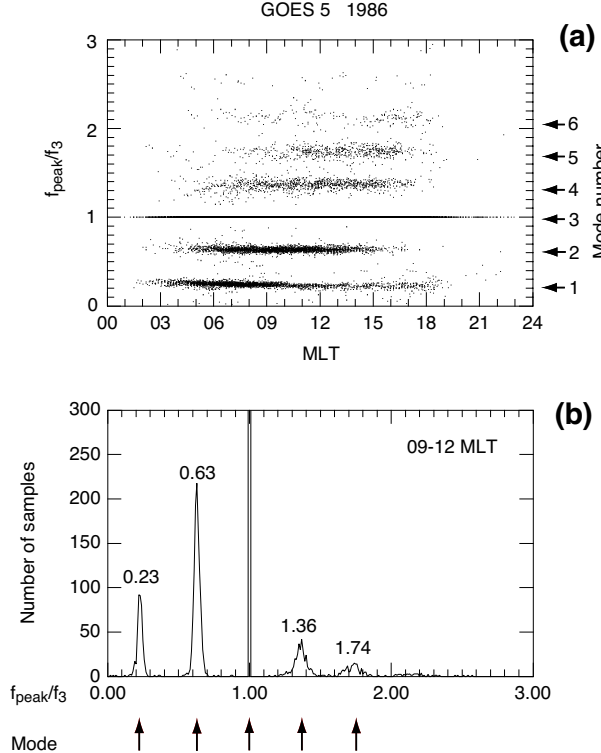
(Angerami and Carpenter, 1964)

It is possible to construct models with more free parameters

Model with 3 free parameters

$$\log_{10} \rho = c_2 \tau^2 + c_4 \tau^4 + c_6 \tau^6$$

$$\tau = \int ds/B$$

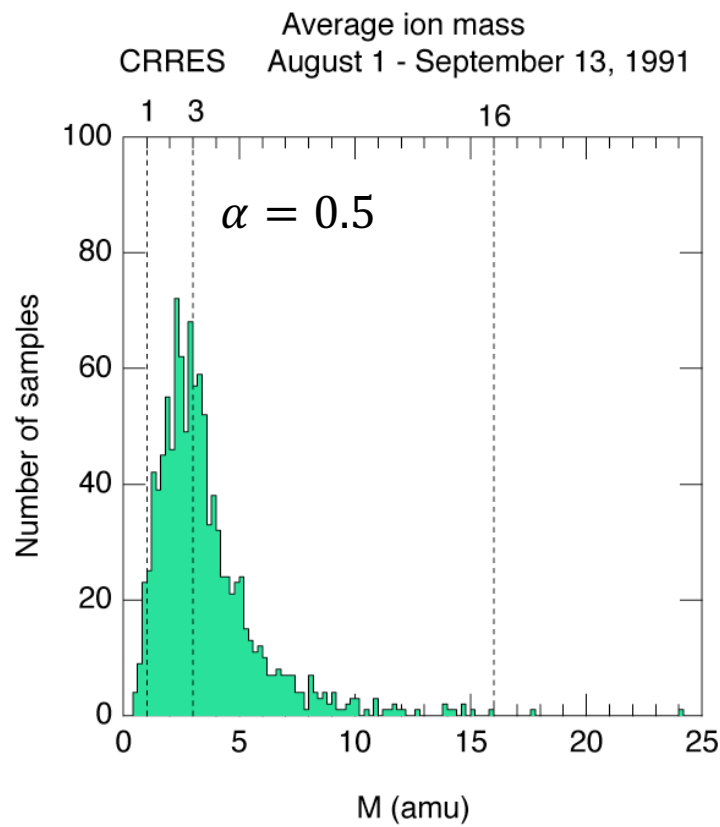
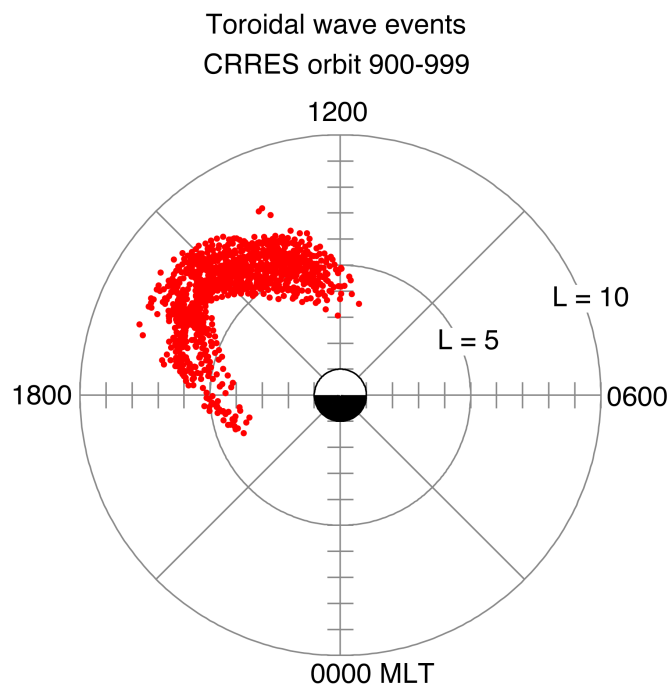


(Takahashi and Denton 2007)

Data Analysis Results

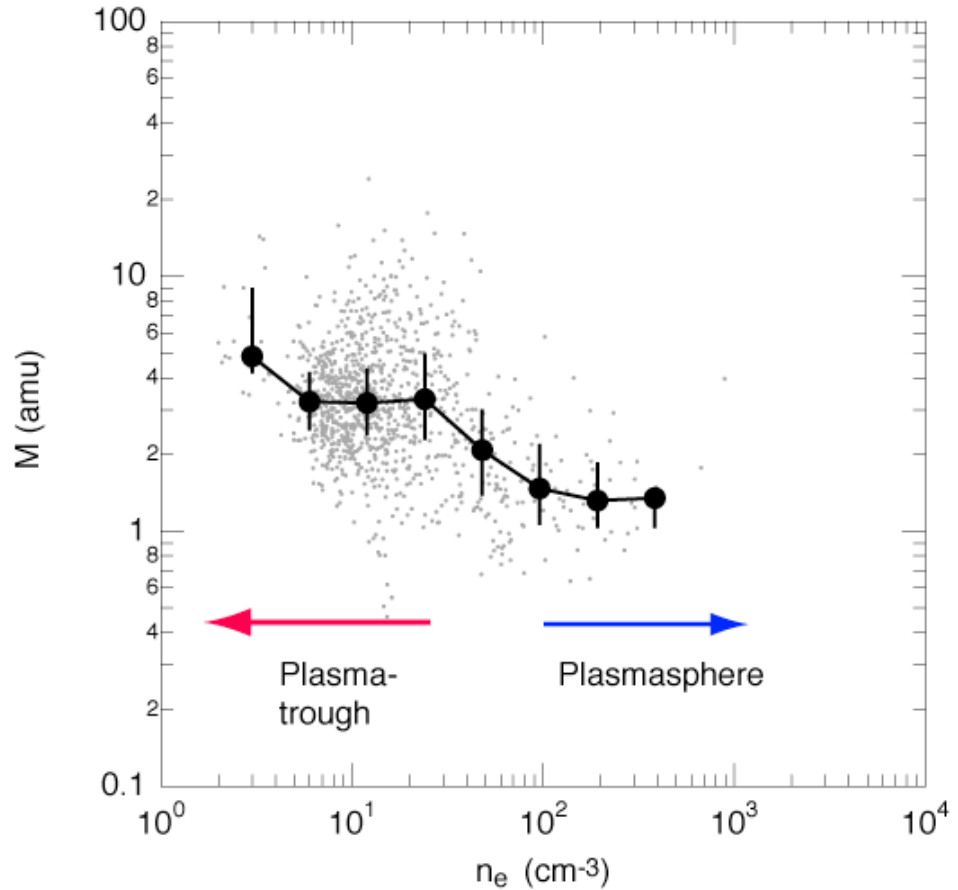
1. CRRES and GOES

Most M estimates are in the physically reasonable range
1 (all-H⁺) -16 (all-O⁺) amu



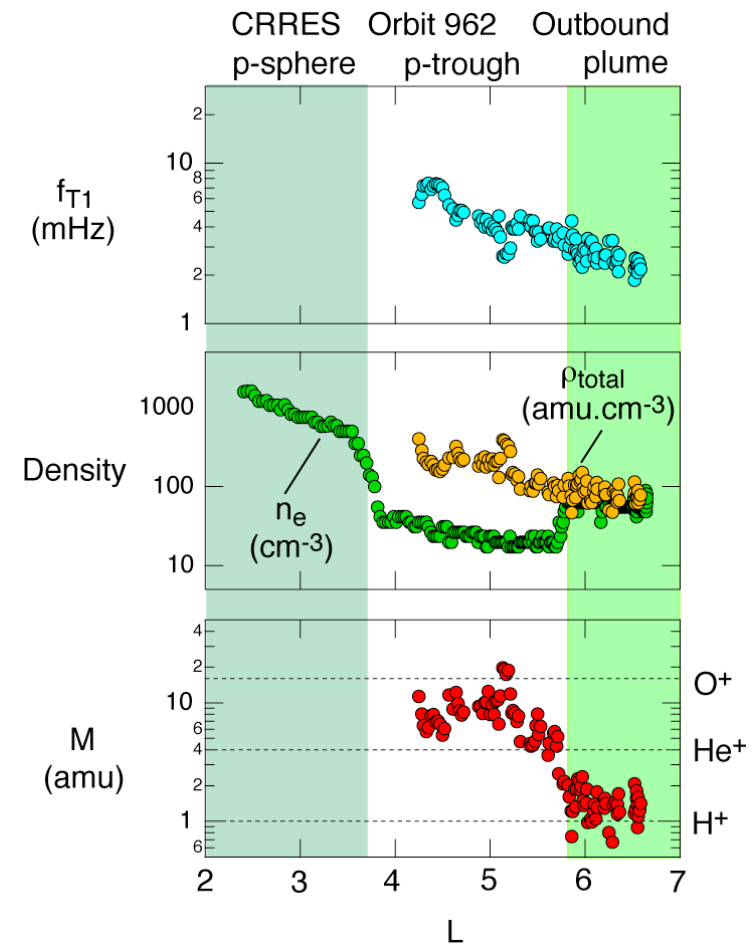
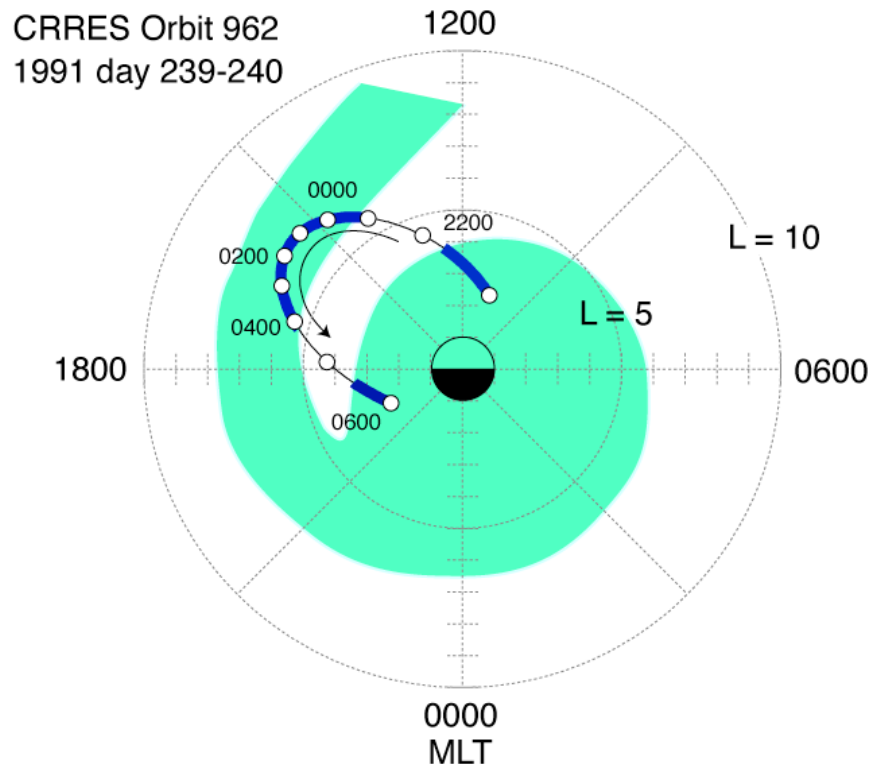
M (plasmasphere) < M (plasmatrough)

- M depends on electron density:
 - High (> 2 amu) when n_e is low (plasmatrough)
 - Low (< 2 amu) when n_e is high (plasmasphere)
- If $[\text{H}^+, \text{O}^+]$ plasma
 - 13% O^+ in the plasmatrough

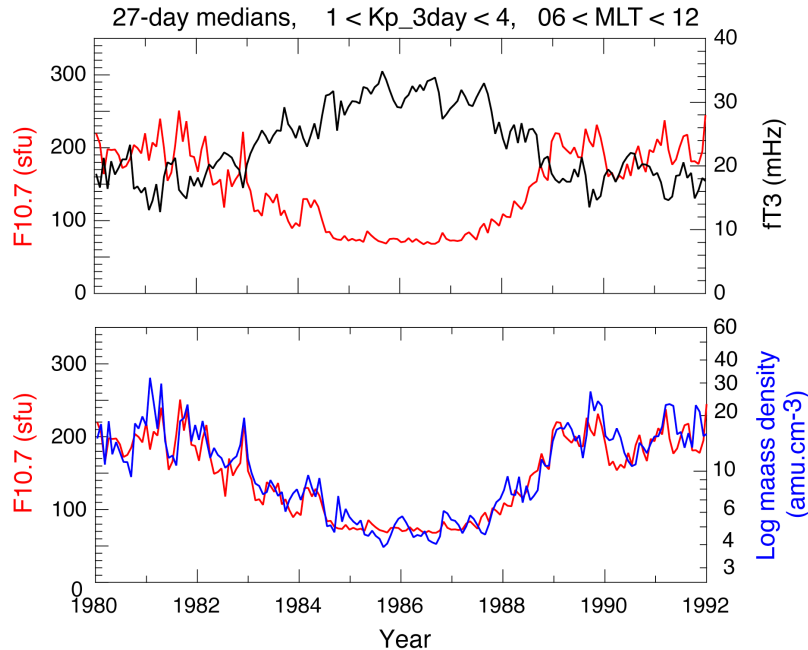


(Takahashi et al., 2006)

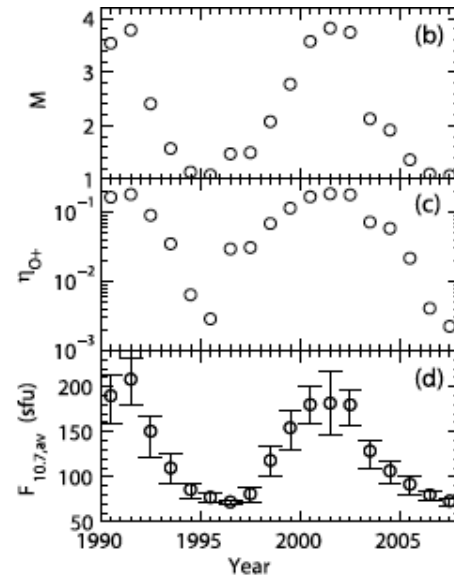
Plume disappears when the mass density is considered



Radiation from the sun is a major controlling factor of O⁺ and mass densities



(Takahashi et al., 2010)



(Denton et al., 2011)

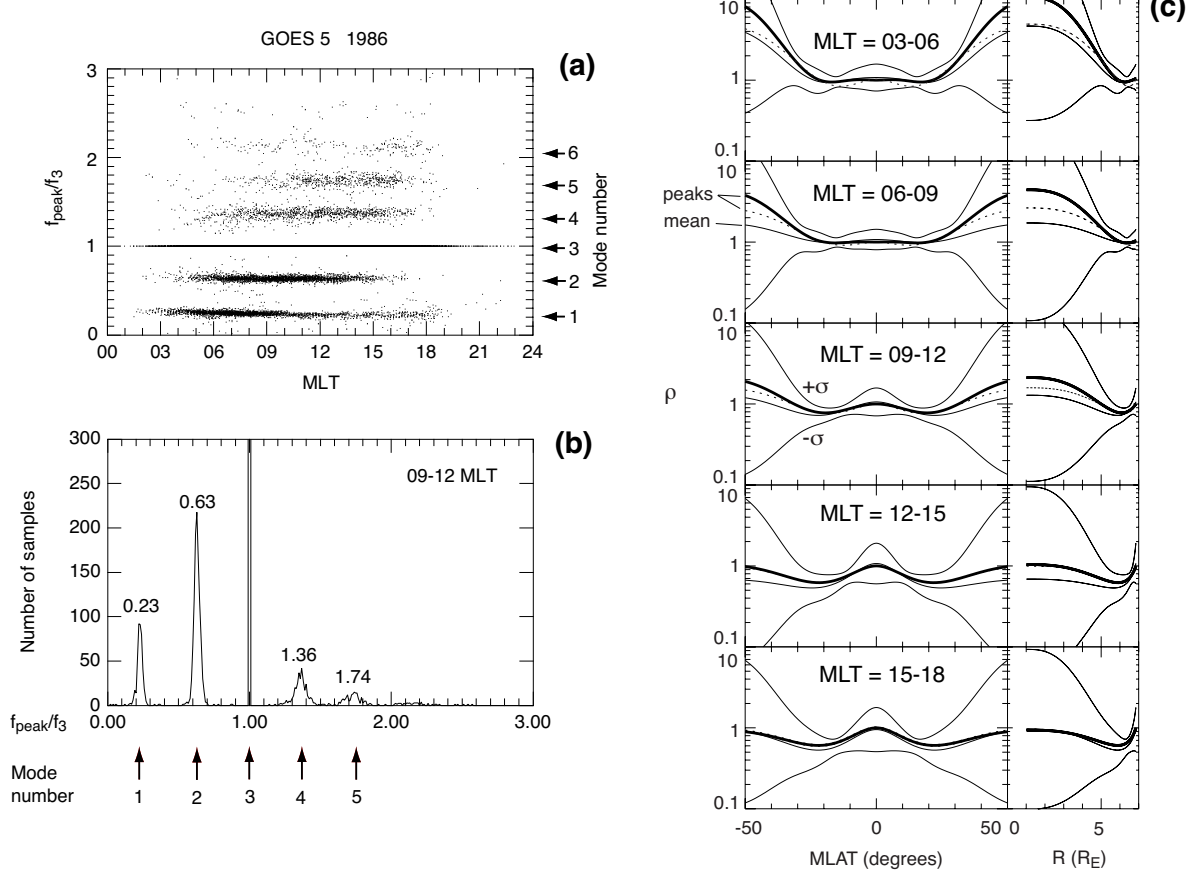
- Mass density changes by a factor of ~4
- Ionospheric heating is the cause of elevated O⁺ during high solar activity

Equatorial mass density peak has been inferred

Model with 3 free parameters

$$\log_{10} \rho = c_2 \tau^2 + c_4 \tau^4 + c_6 \tau^6$$

$$\tau = \int ds/B$$



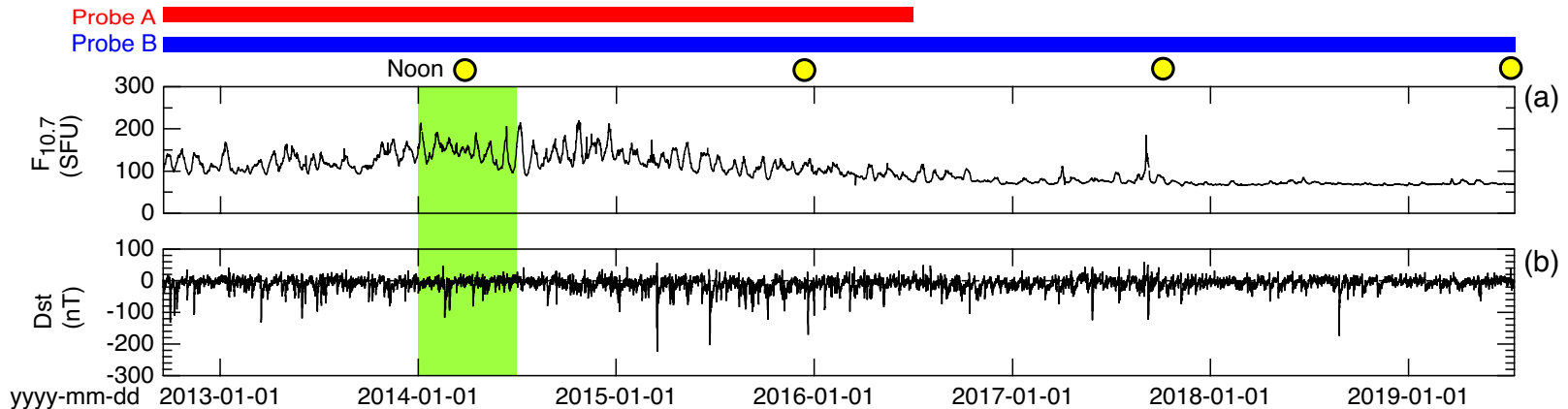
(Takahashi and Denton 2007)

Data Analysis Results

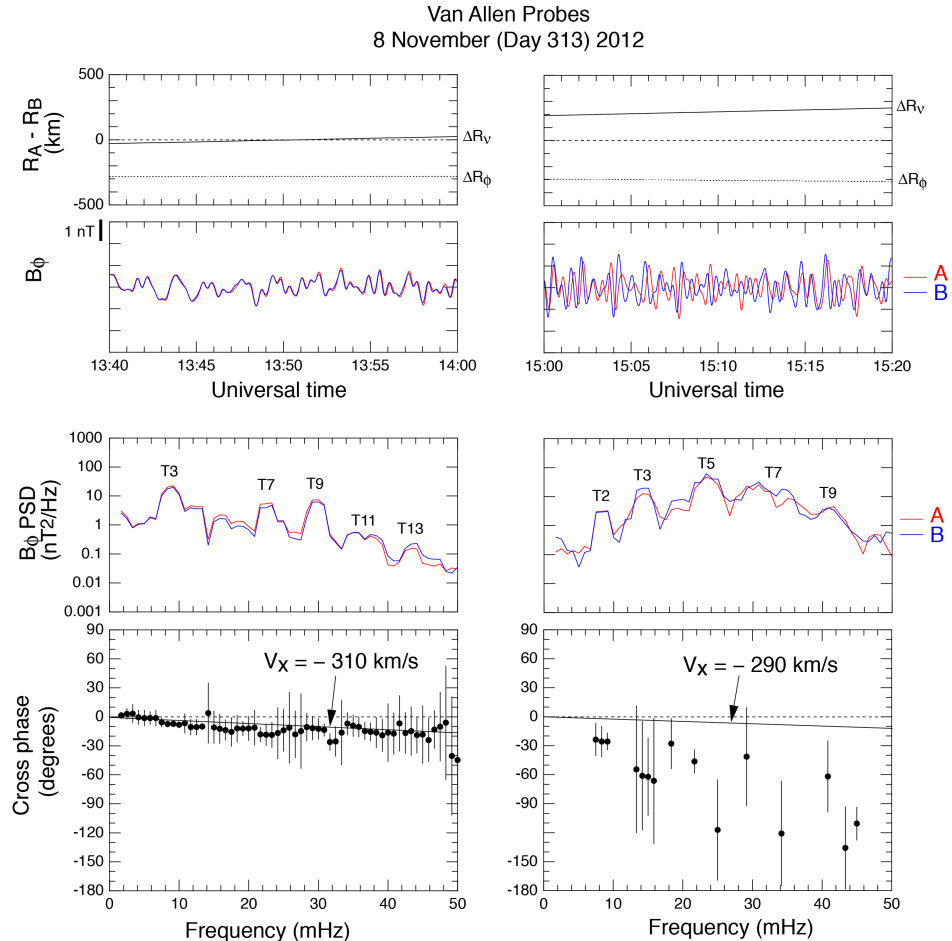
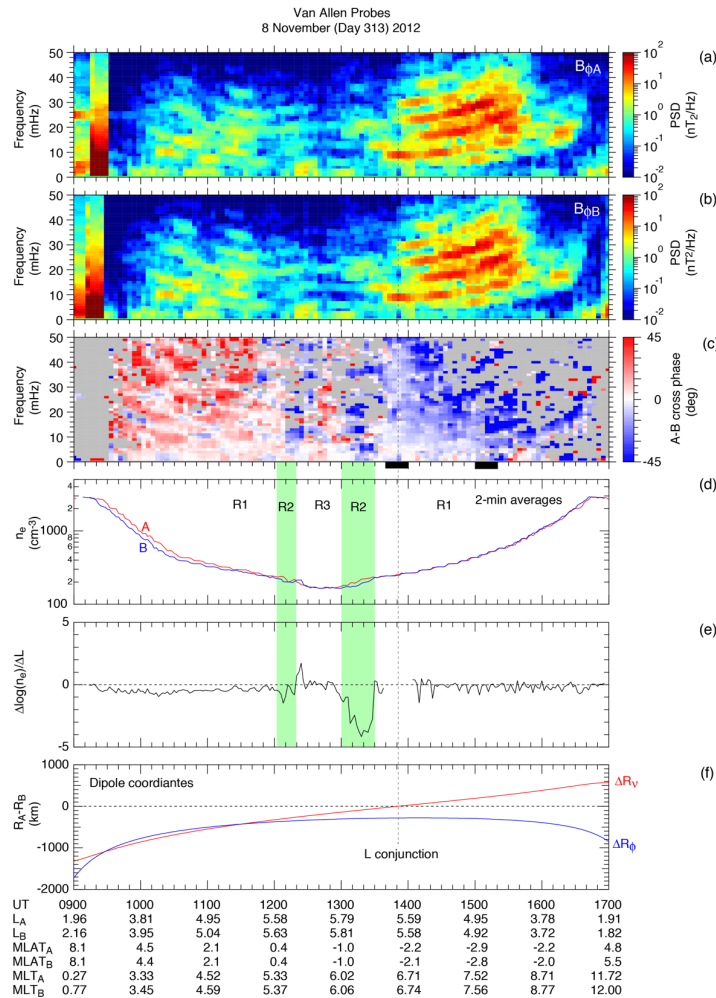
2. Van Allen Probes (RBSP)

Van Allen Probes

- Operated 7 years
- 4 precessions in local time
- Wide range of Solar EUV (F10.7) and Dst
- High-quality E and B data (11-s spinfit), covering several toroidal harmonics

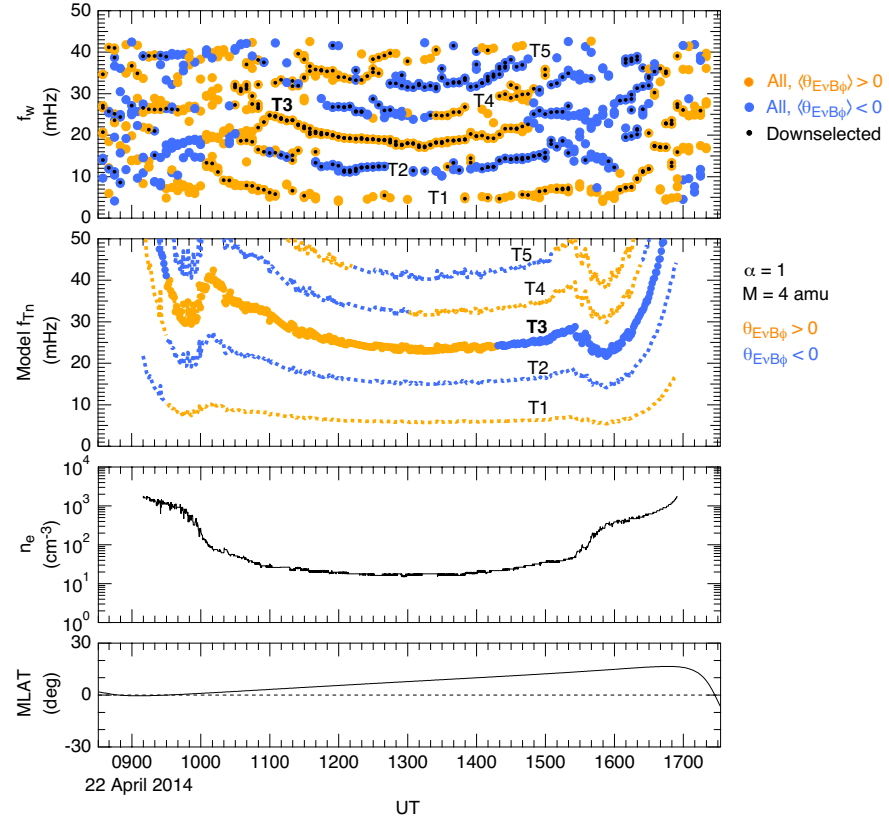
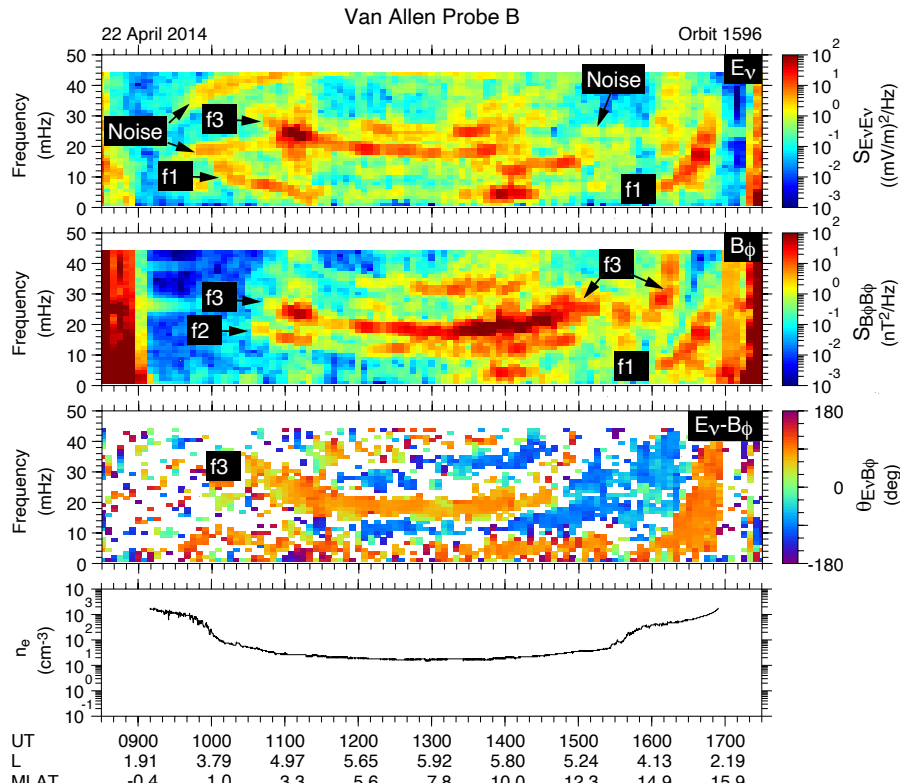


RBSP routinely detect multiharmonic toroidal waves



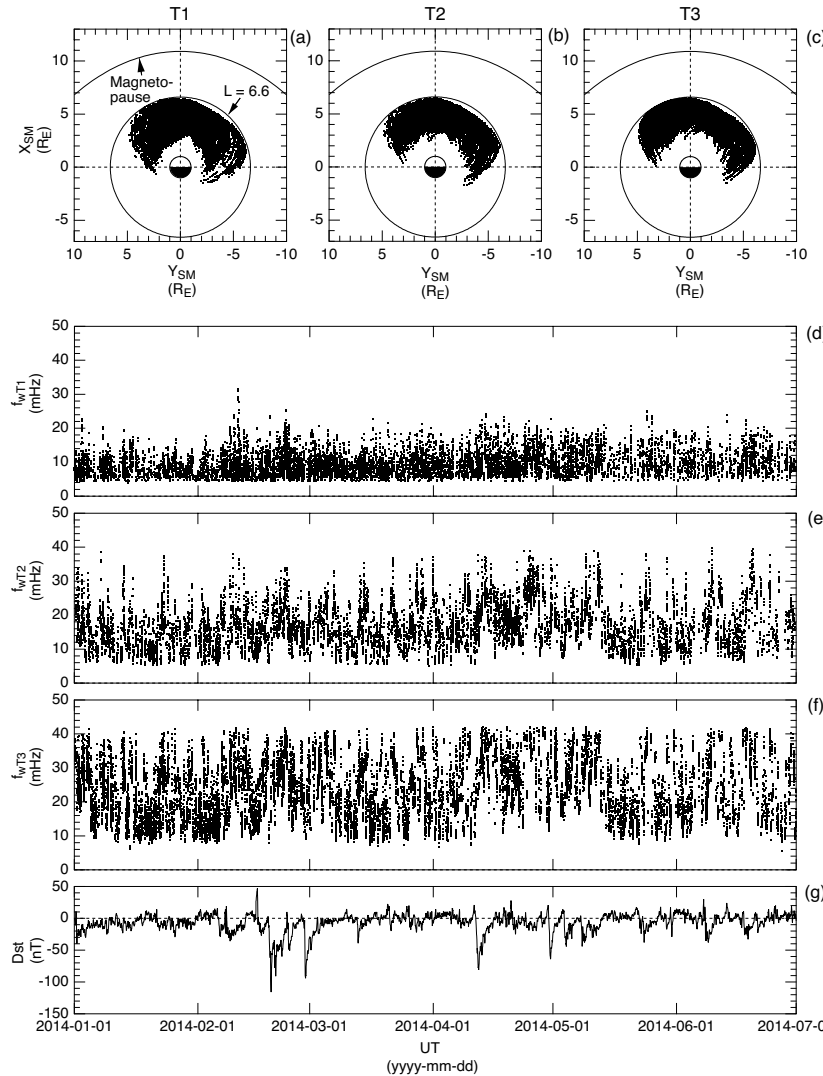
(Takahashi et al., 2015)

We use graphical interface for manual identification of f1, f2, and f3

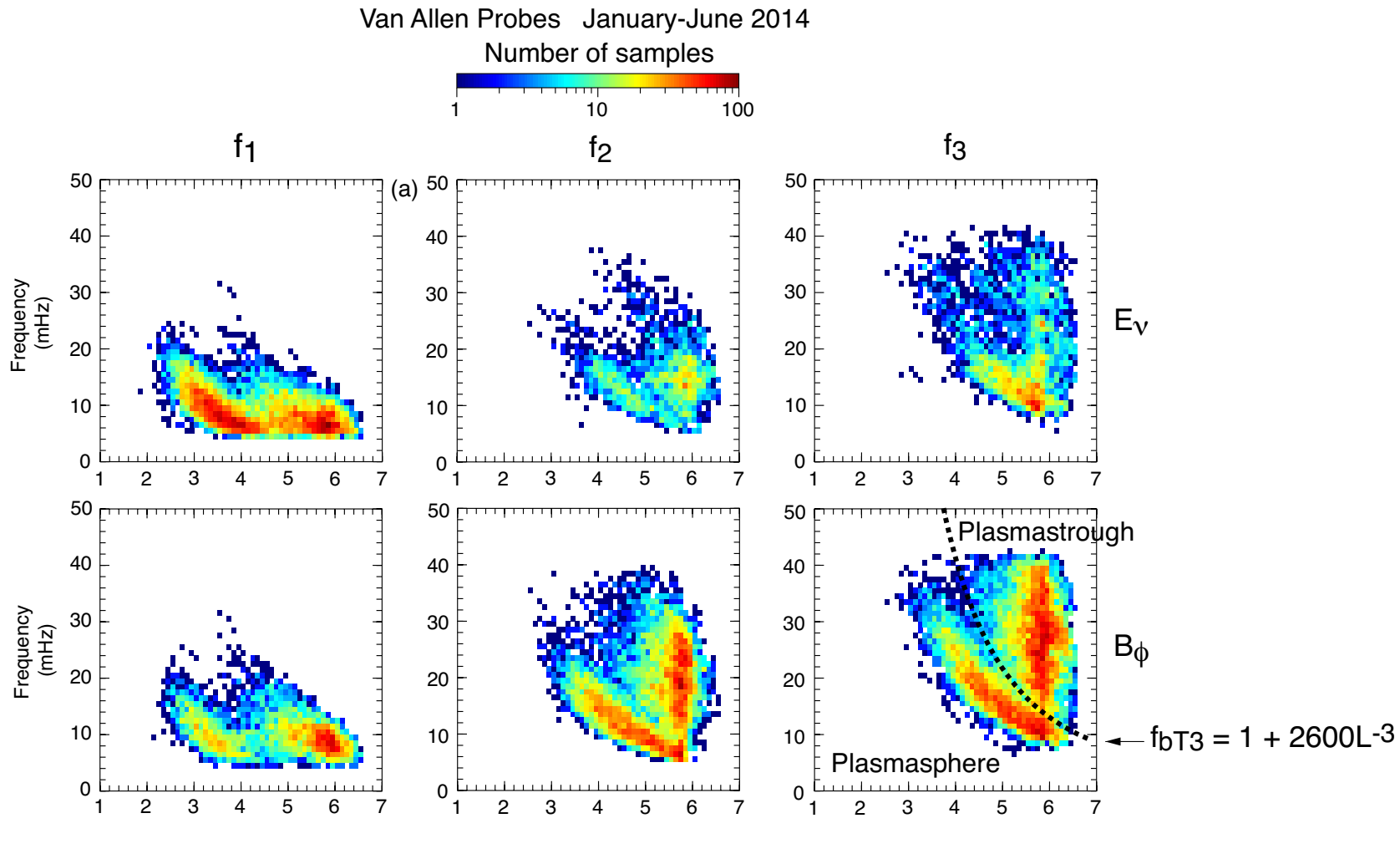


(Takahashi et al., 2015)

Dayside toroidal waves: 6-month statistics

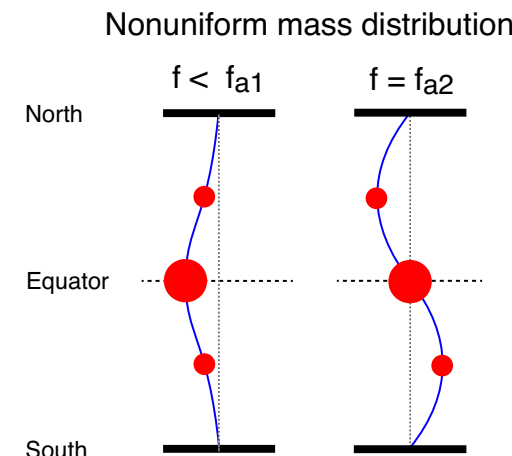
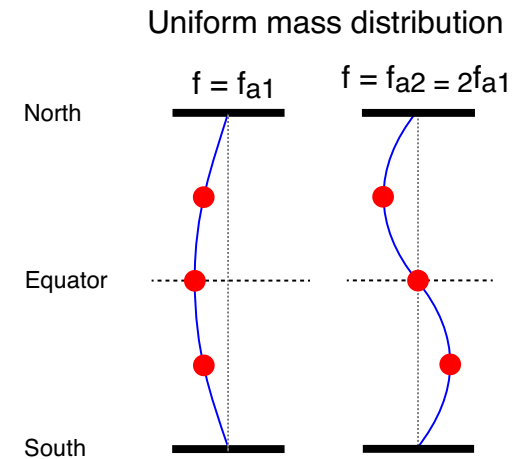


L distribution of wave frequency shows distinction between regions

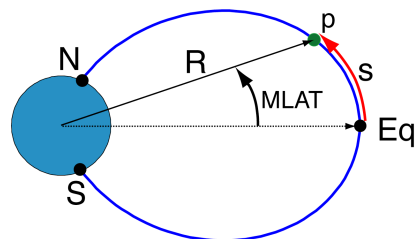


Field line mass distribution controls the harmonic frequencies and node latitudes

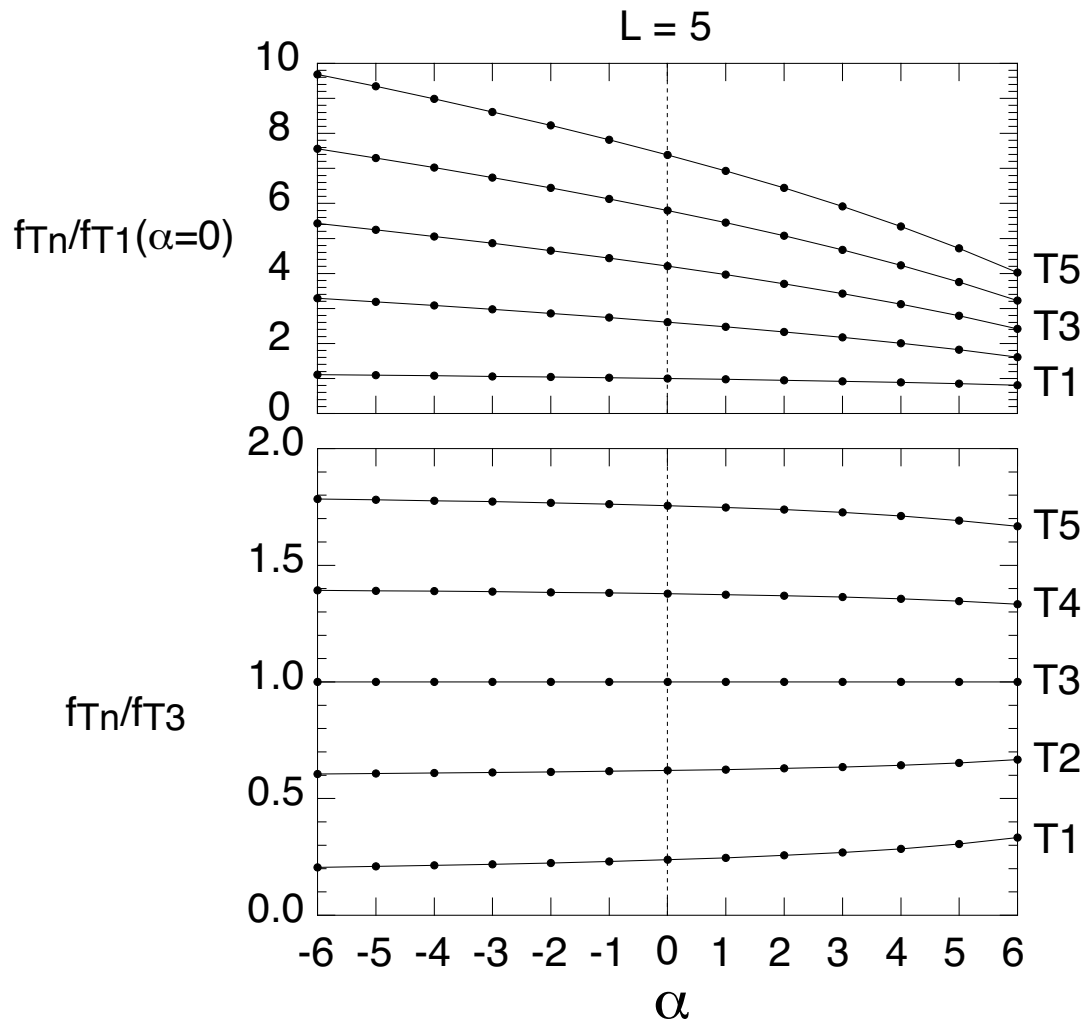
- The frequency and mode structure of standing waves depends on the field line mass distribution
- More observable harmonics means more density model parameters (inversion)
 - $N < 10$, realistically, not quite like helioseismology
- Spacecraft measurements are better suited than ground measurements.
 - Frequently yield several harmonics



α can be determined using the frequency ratios between harmonics



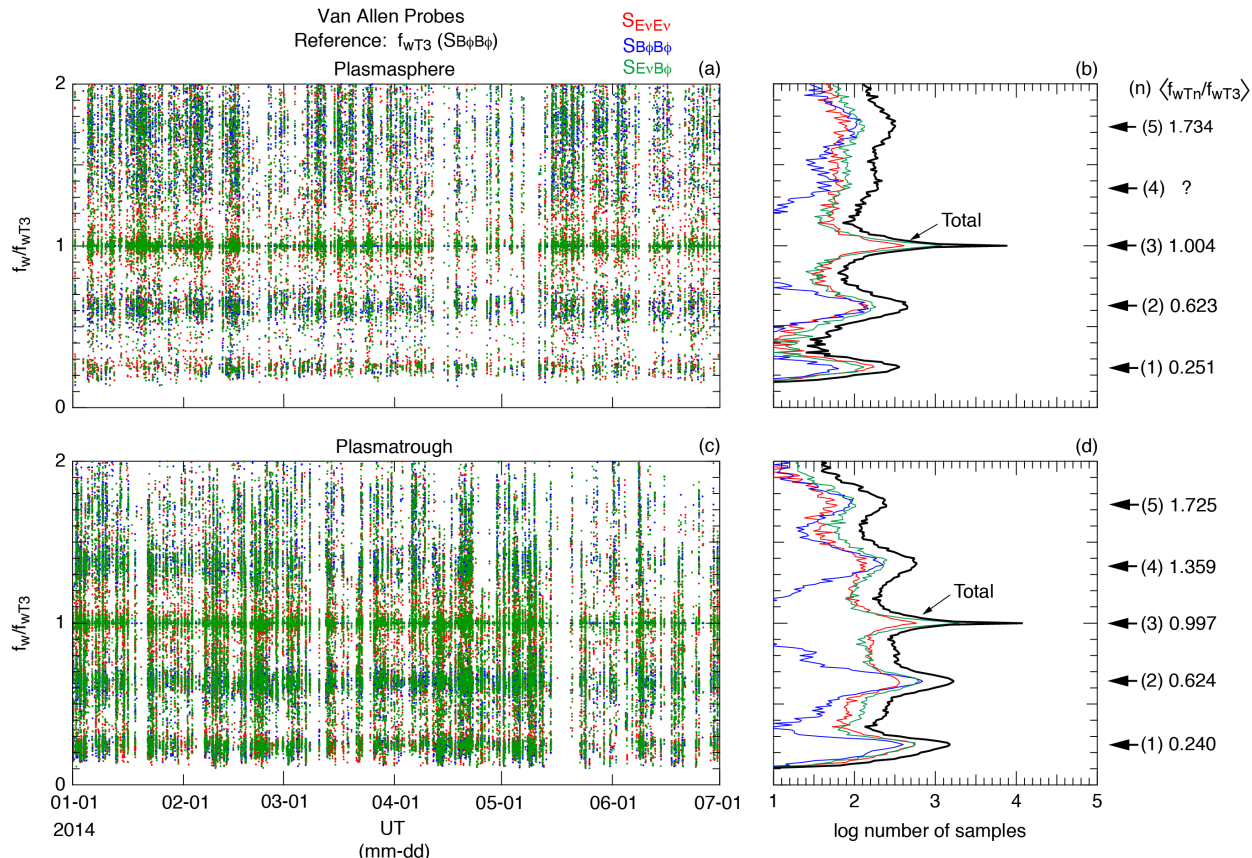
$$\rho = \rho_{eq} \left(\frac{LR_E}{R} \right)^\alpha$$



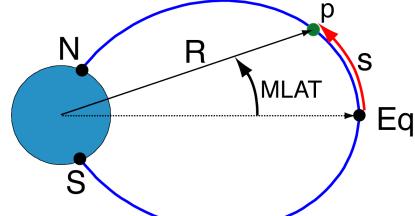
Frequency distribution

Normalized to the third harmonic frequency (f_3) detected in the B_ϕ spectrum

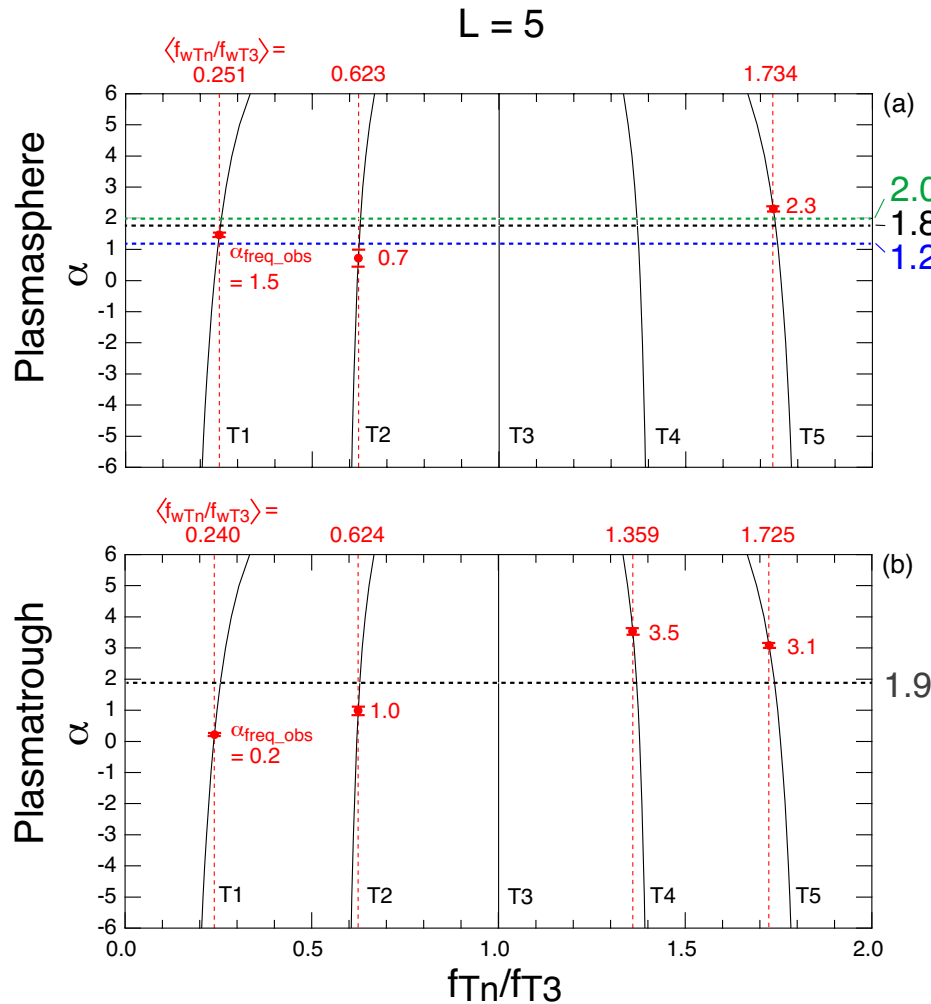
Plasmasphere



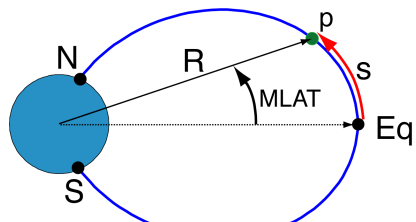
α can be determined using the frequency ratios between harmonics



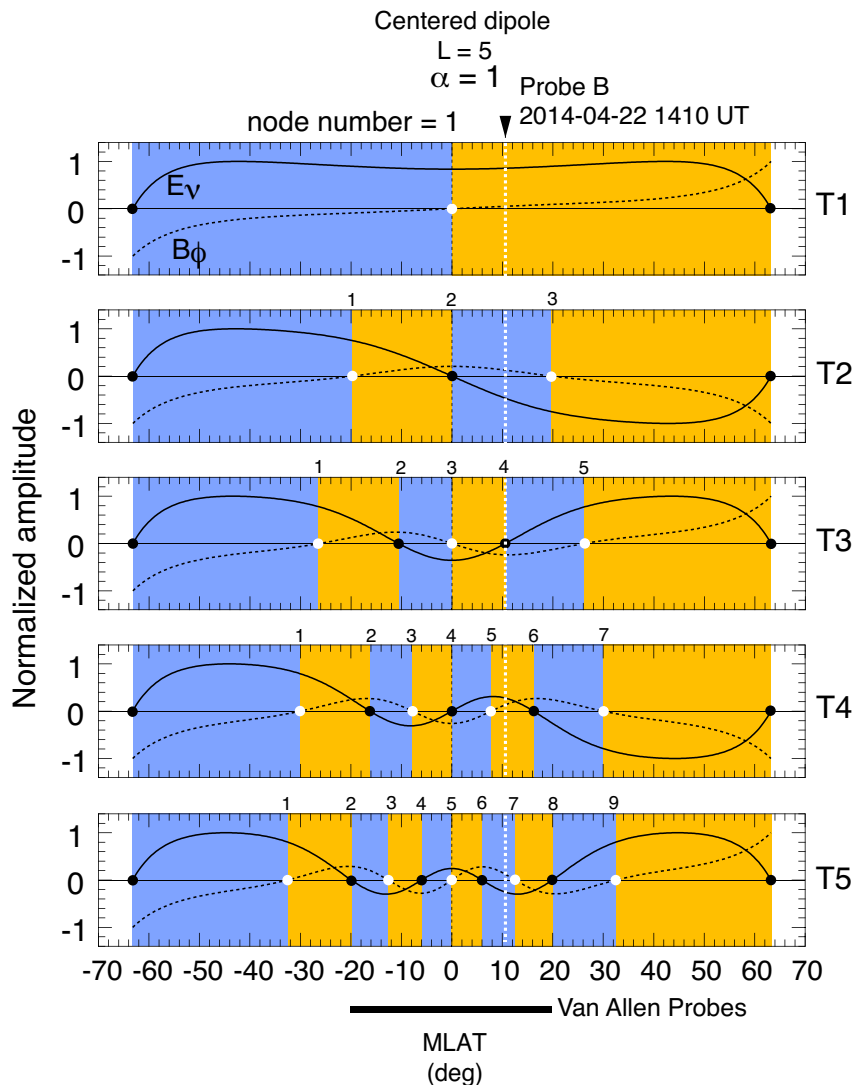
$$\rho = \rho_{eq} \left(\frac{LR_E}{R} \right)^\alpha$$



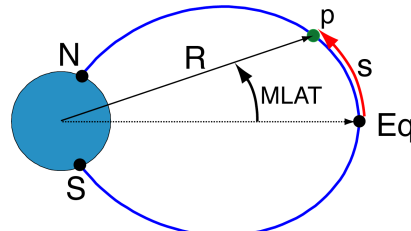
Theoretical mode structures along the field line



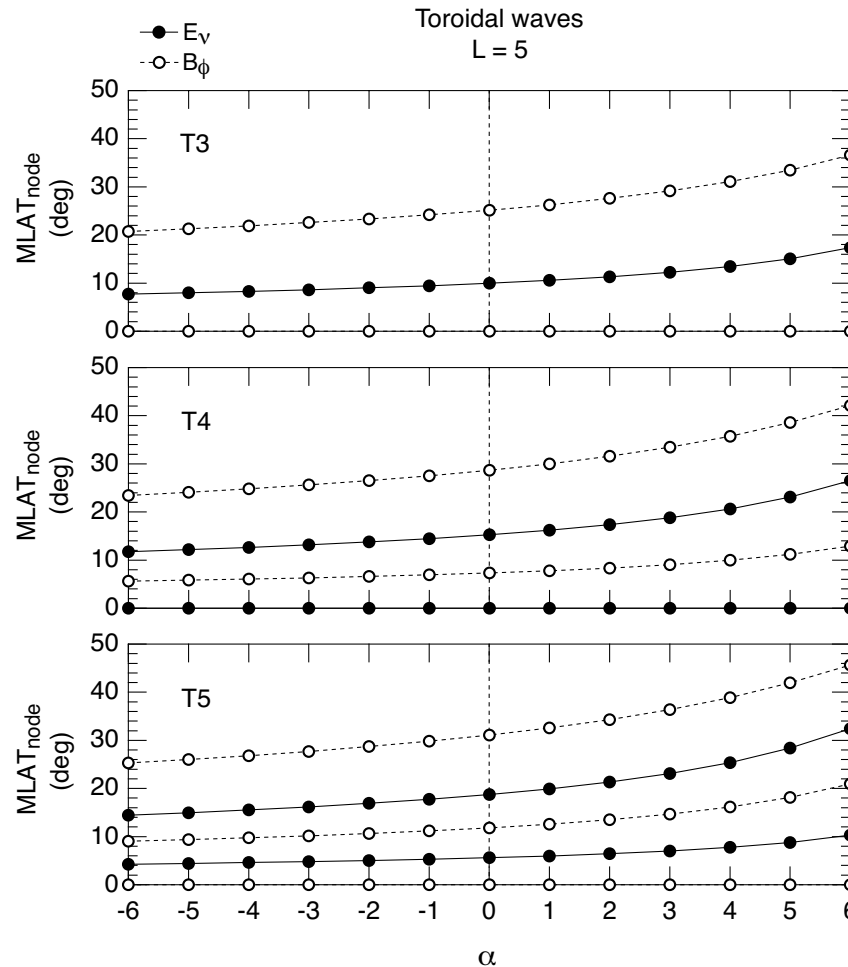
$$\rho = \rho_{eq} \left(\frac{LR_E}{R} \right)^\alpha$$



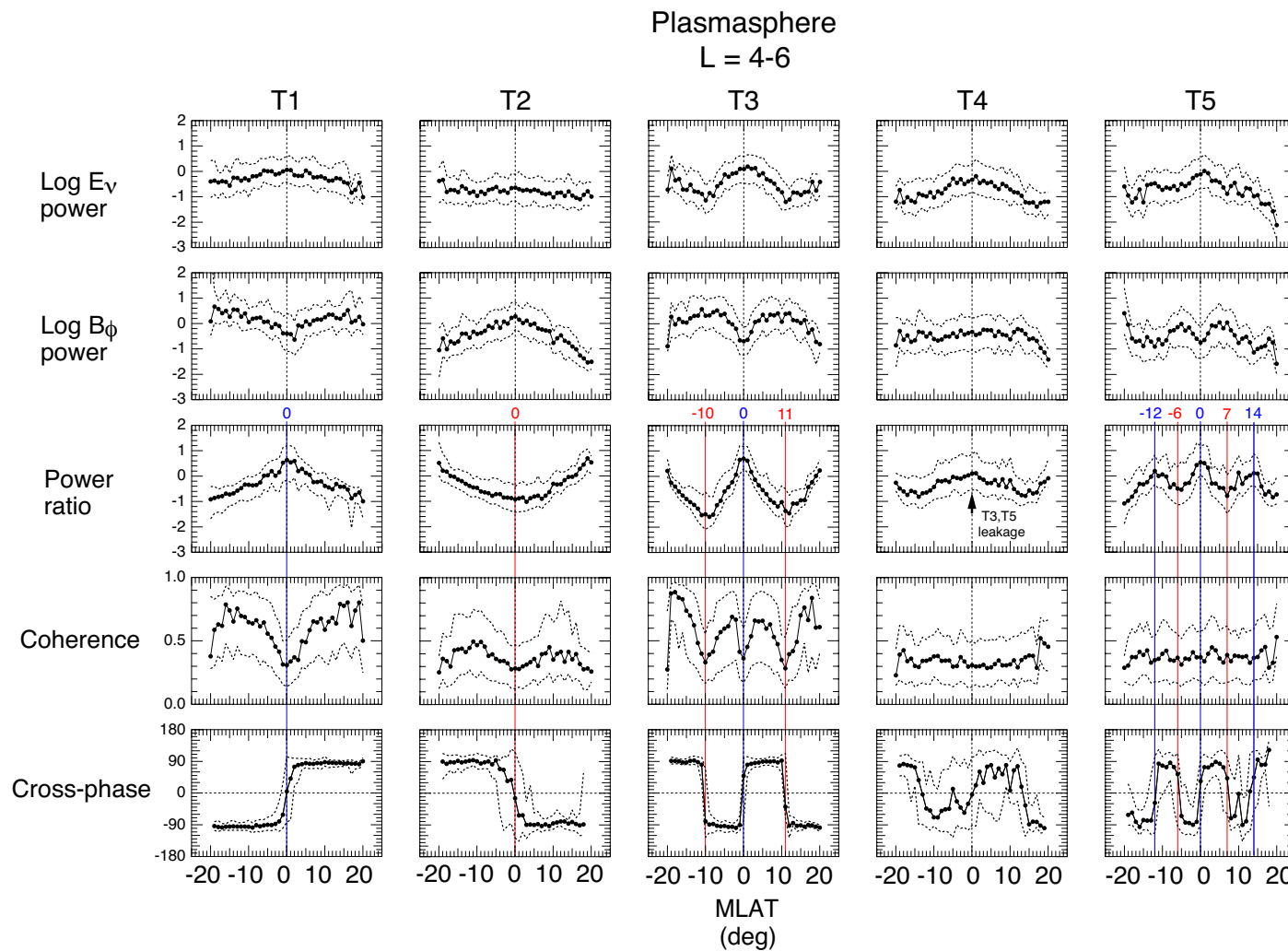
α can be determined using the latitudes of observed nodes



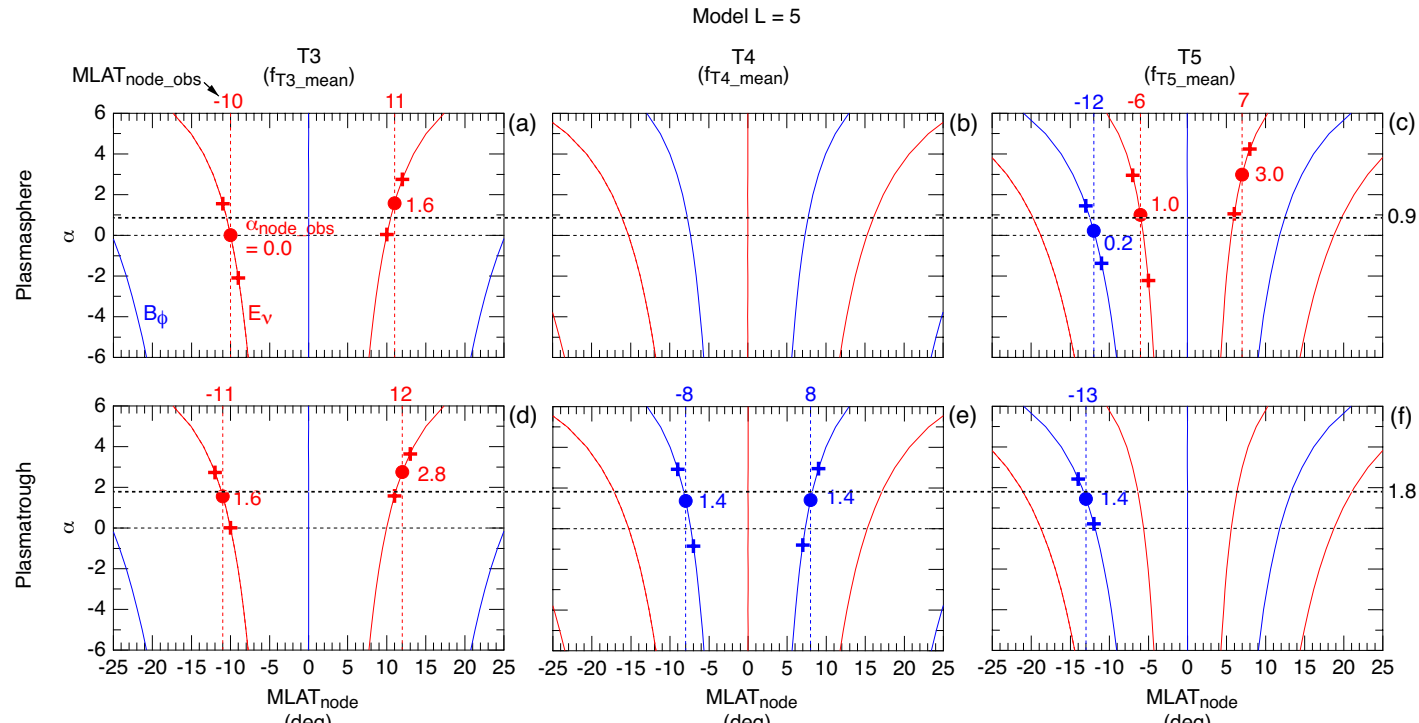
$$\rho = \rho_{eq} \left(\frac{LR_E}{R} \right)^\alpha$$



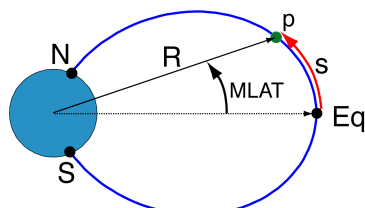
Toroidal wave mode structure



Estimating α from observed node latitudes



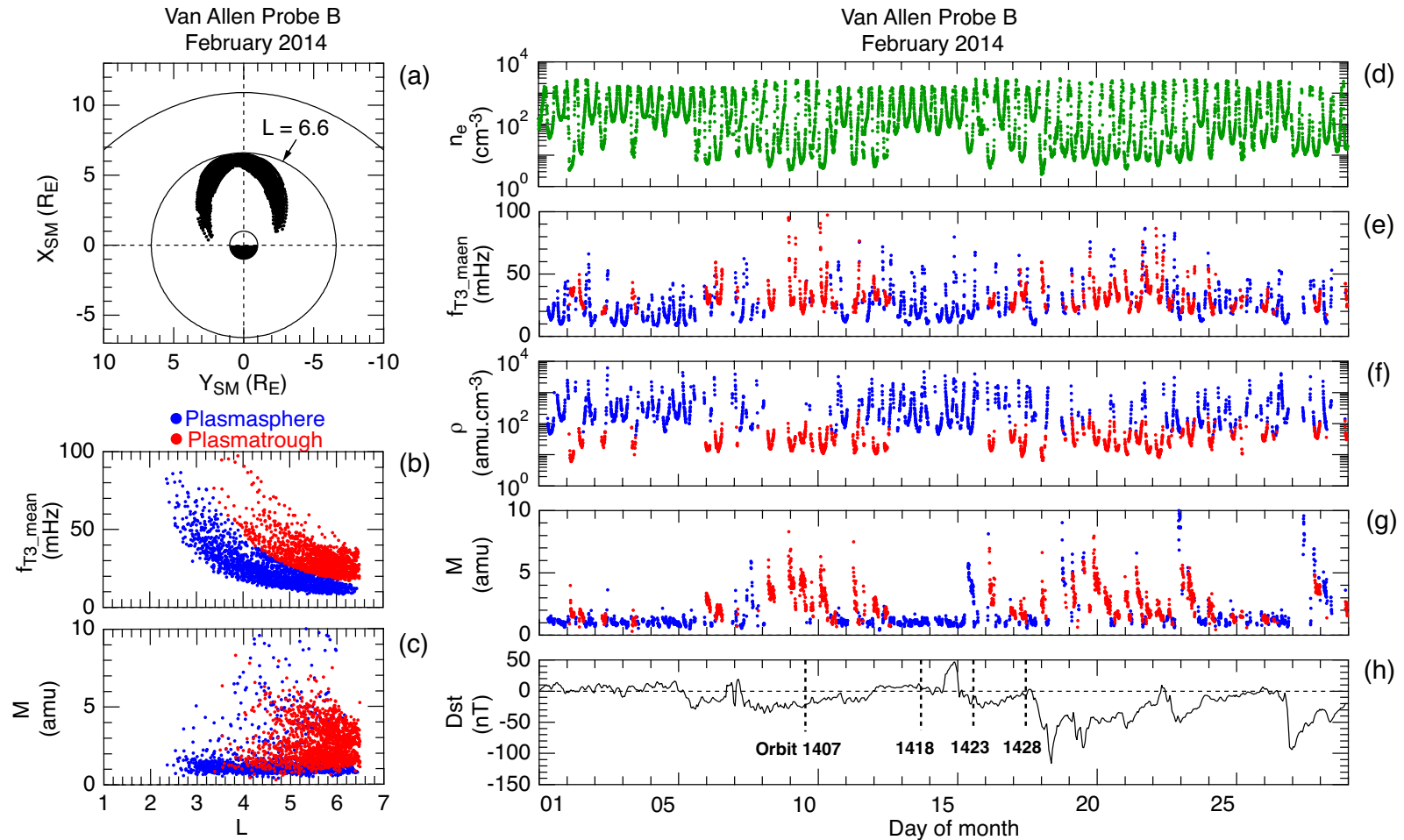
Takahashi and Denton (2021)



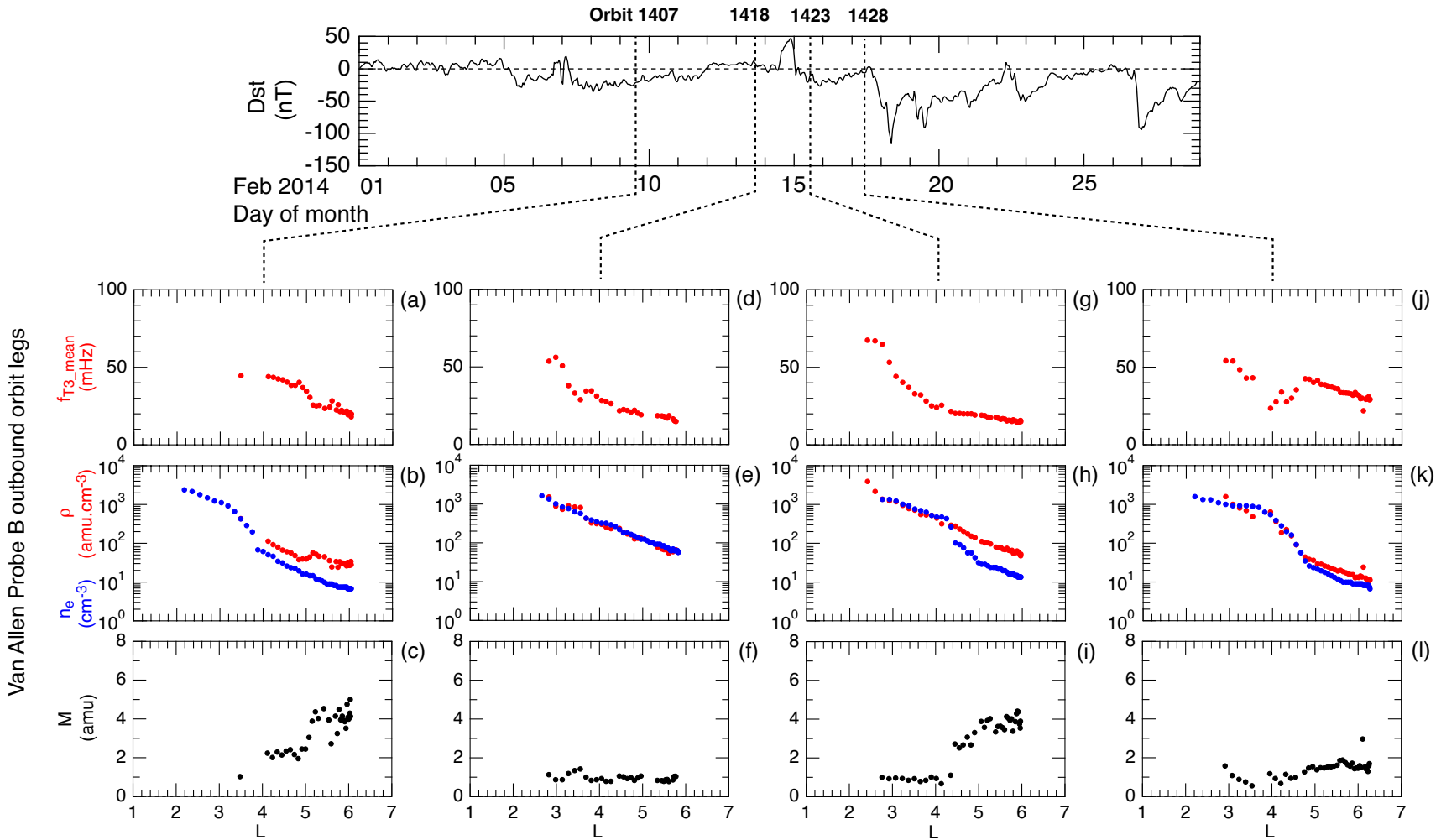
$$\rho = \rho_{eq} \left(\frac{LR_E}{R} \right)^\alpha$$

$\alpha \sim 1$ (plasmasphere)
 $\alpha \sim 2$ (plasmatrough)

February 2014 summary plots: Mass density and average ion mass

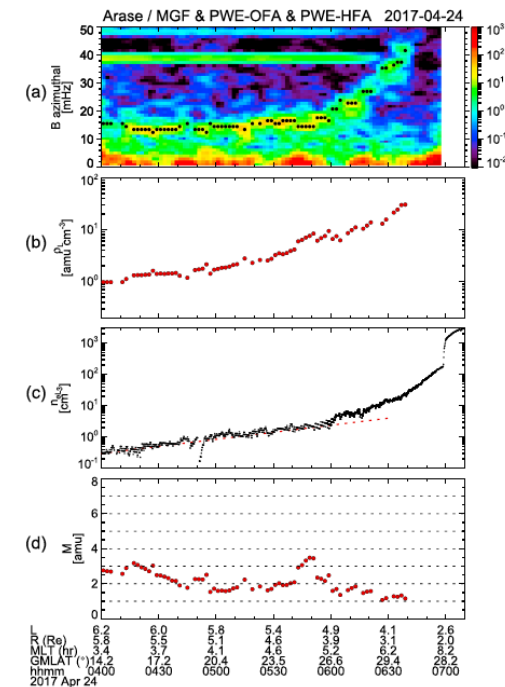
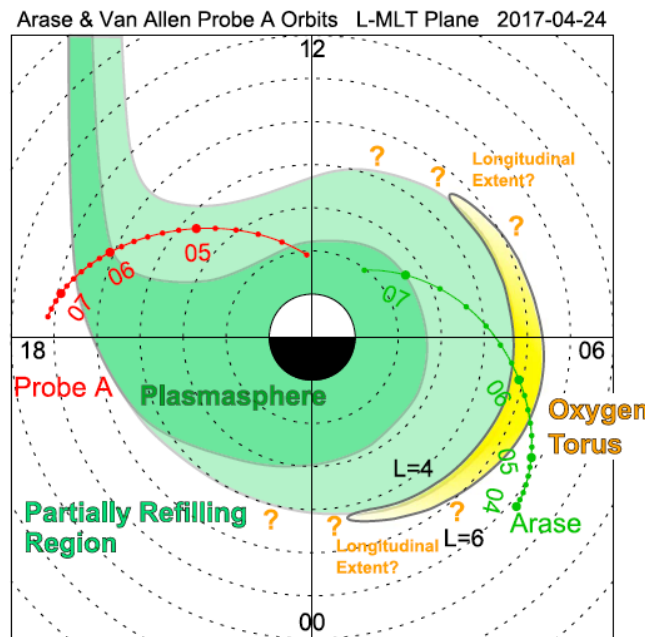
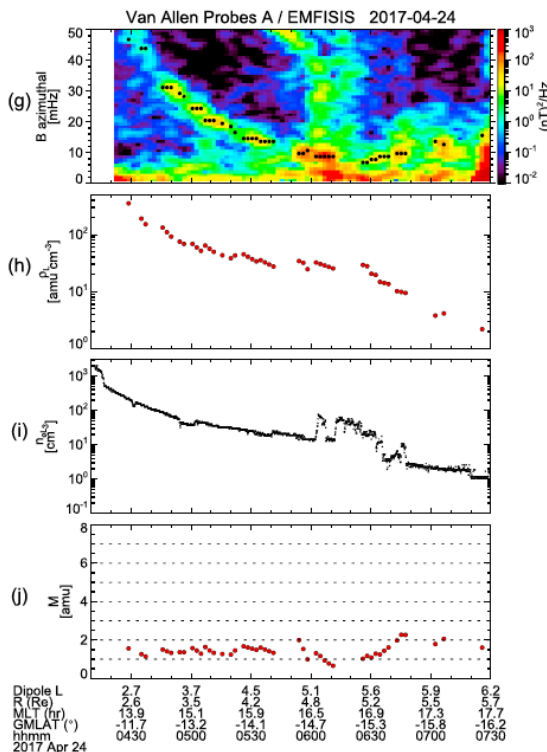


Radial profiled of M is highly dependent on geomagnetic activity



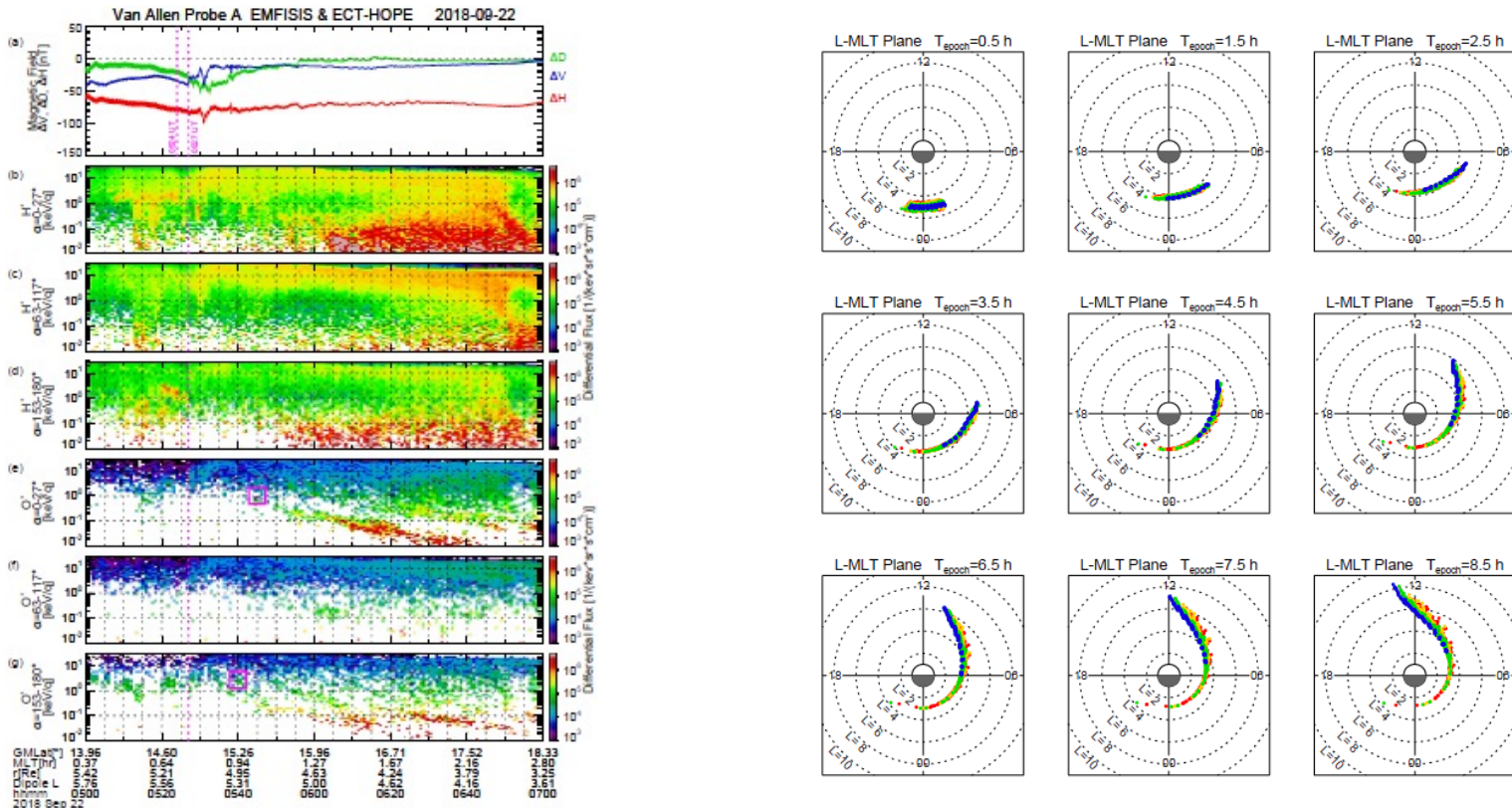
Arase-RBSP Case study suggests partial O+ torus

(Partial) Oxygen torus



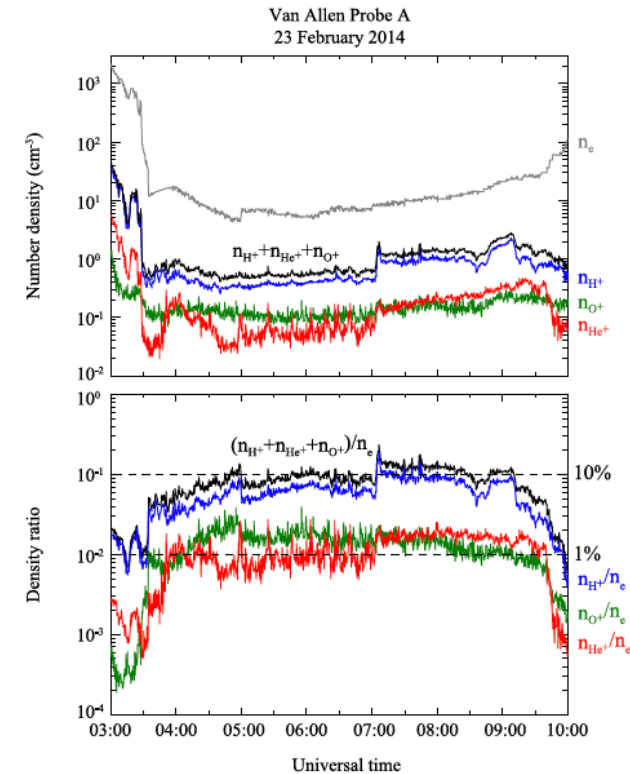
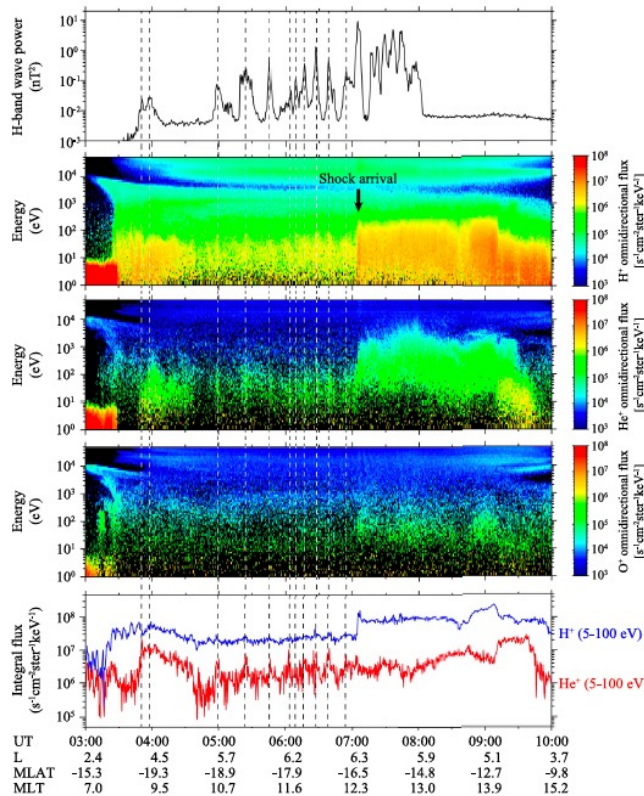
(Nosé et al., 2018)

Field-aligned low-energy O⁺ ions generated at substorm may be the source of partial O⁺ torus



(Nosé et al., 2022)

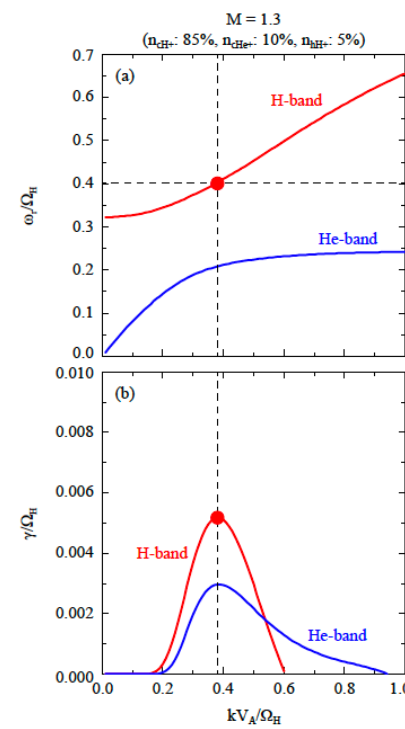
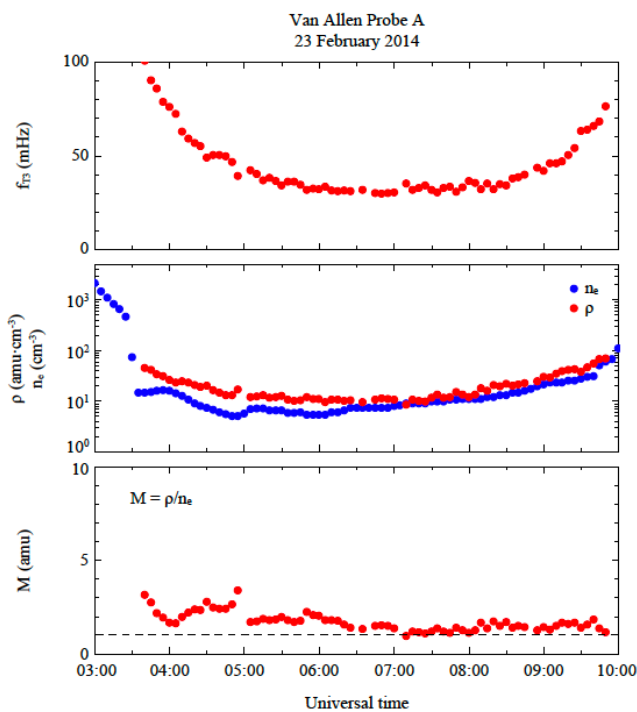
Magnetoseismology contribution: Growth rate of EMIC waves



(Kim et al., 2022)

Magnetoseismology contribution: Growth rate of EMIC waves

The average ion mas can constrain the O⁺ density, which affects the growth rate



(Kim et al., 2022)

Work in progress

- Solar cycle variation of the average ion mass
- Spatial structure of the O⁺ -rich region and its dependence on geomagnetic activity
- Model of the mass density and average ion mass